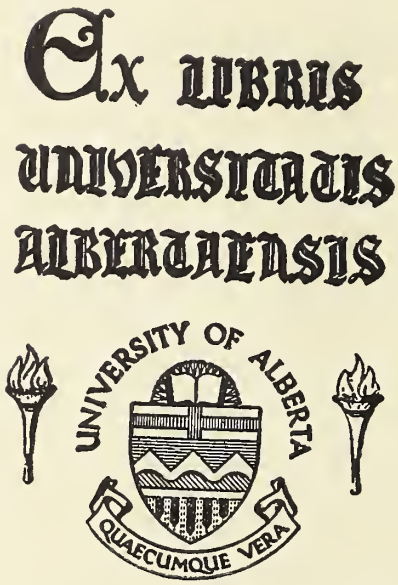

THE UNIVERSITY OF ALBERTA

PHOTOCONDUCTIVITY OF MONOCRYSTALLINE CUPROUS OXIDE

A THESIS

SUBMITTED TO THE FACULTY OF GRADUATE STUDIES

IN PARTIAL FULFILLMENT OF THE REQUIREMENTS FOR THE DEGREE

OF MASTER OF SCIENCE

DEPARTMENT OF PHYSICS

BY

EMERY R. FORTIN

Edmonton, Alberta

April, 1962

TABLE OF CONTENTS

FIGURES

LIST OF TABLES

ACKNOWLEDGMENTS

I would like to thank:

Dr. Frank L. Weichman for introducing the problem to me and for his steadying guidance throughout the course of my work;

Mr. Jack Legge, for patiently doing most of the glass work required by this experiment;

Mr. Walter Corfield, for building the pre-amplifier, and helping to solve some of the electronics problems involved in the experiment;

Mr. Philip Crouse, for performing some of the precision work on the sample holder;

Mr. Bruce Maxfield, for valuable help, in the early stages of the experiment.

ABSTRACT

This thesis describes experiments performed in order to determine the photoconductivity of monocrystalline cuprous oxide. Single crystals of Cu_2O of orientation $\{3, 1, 1\}^*$ were grown in the laboratory, and their conductivity characteristics were studied beforehand. A mosaic structure crystal, of the type studied by previous investigators, was also studied for sake of comparison. It was found that both types of crystals had essentially the same photoconductive properties. From this fact, it is concluded that the crystalline structure plays a minor role in the photoconductivity of cuprous oxide: the content of excess copper or excess oxygen in the lattice is still the major factor governing the properties of this semiconductor.

* $\{3,1,1\}$ planes are in the plane of the slab.

I. INTRODUCTION

It was in 1873 that Willoughby Smith, in the United States, disovered that selenium increases in conductivity upon illumination. The phenomenon was named photoconductivity. From then on, numerous other materials were found to be photoconductive, e.g. thallous sulphide, lead sulphide, silicon, cuprous oxide.

This last compound, cuprous oxide, has been extensively investigated for more than fifty years. This semiconductor shows luminescence, electroluminescence and photoconductivity. The photoconductivity of cuprous oxide was first studied by Pfund (1916), and by numerous other investigators up to now. However, a survey of the literature shows that there are considerable variations between the results found by different authors. All the investigations up to the present time have been made on polycrystalline samples, containing, most of the time, considerable amounts of excess oxygen. It is believed that imperfections in the structure and composition of the samples studied by previous investigators, were responsible for the variations in their findings.

The purpose of the present work is to study the photoconductivity of single crystals of cuprous oxide, grown in the laboratory, under very specific conditions. Working on a single crystal removes to a great extent the discrepancies due

to grain boundaries, or other structural imperfections. Secondly, keeping the composition of the sample very close to stoichiometric proportions allows one to obtain definite and reproducible results.

In the present work, we first describe in details the experimental procedure used for crystal growing, and for resistivity and photoconductivity measurements. This is followed by a few pages on conductivity itself. Some theoretical ideas pertaining to photoconductivity are then developed, and a survey of the literature on the subject is presented. Finally, our own results are given, and interpreted on the basis of a simple band model.

II. EXPERIMENTAL PROCEDURE

A. Preparation of Samples

The equipment used to prepare the cuprous oxide samples is shown in Fig. 1. A Symplytrol pyrometer with a chromel-alumel thermocouple as a sensing element served to keep the temperature in a Kanthal wound oven constant within about ten degrees Centigrade of any chosen value by turning on or off the heating current of 9.5 amperes (220 volts). The samples were oxidized inside a McDanel high temperature porcelain tube, which had the property of being able to maintain a vacuum of 10^{-5} mm of Hg at temperatures as high as 1400°C, and was chemically very stable. The necessary vacuum of sufficient flexibility was obtained by the use of a mechanical fore-pump for rough vacuum, or an activated charcoal trap immersed in liquid air for "high" vacuum.

The samples were made from high purity Matthey copper, which had been rolled down to the proper thickness (0.1 to 0.2 mm). The copper was initially annealed in a flame, quenched in cold water, etched in nitric acid and carefully cleaned with distilled water. This process was repeated several times during the rolling down procedure. The shiny sheet of copper was then cut into the proper shape, and placed on a platinum sheet mounted on boats made from the same porcelain material as the large tube, and was heated up to 980°C in "charcoal trap" vacuum.

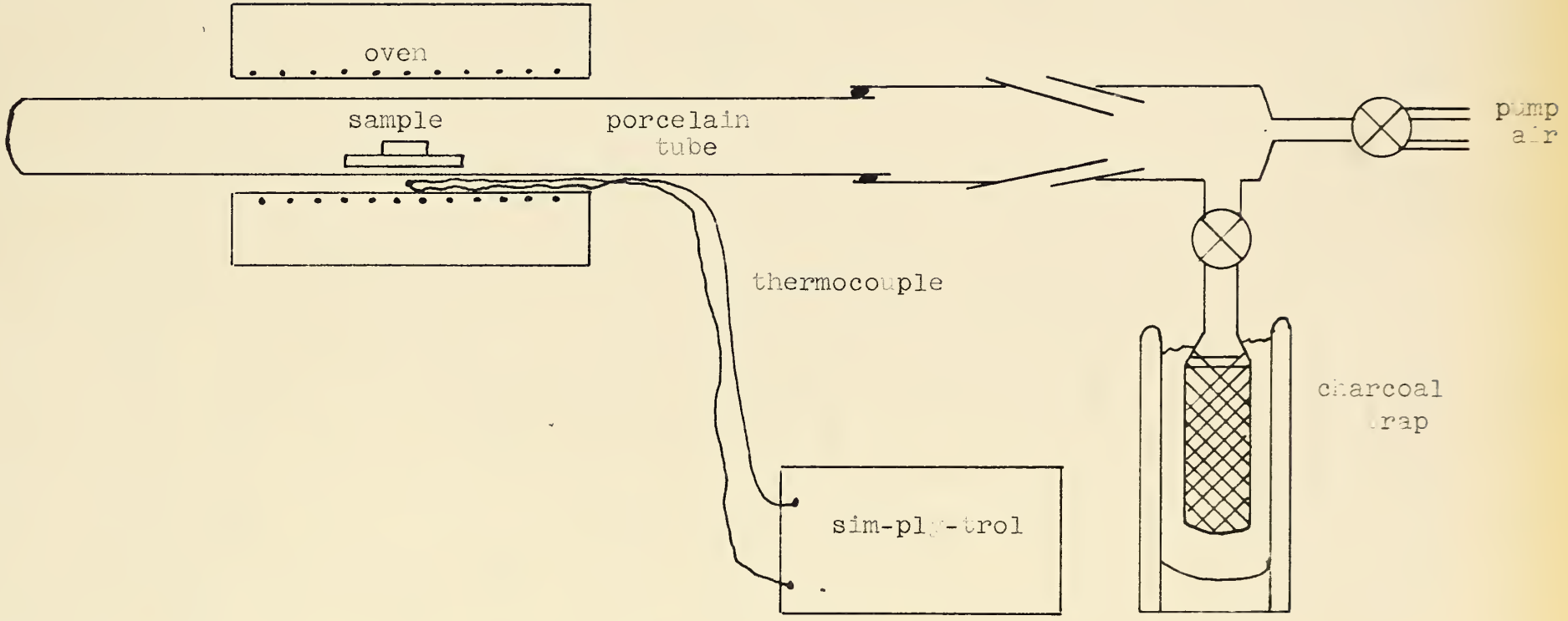

Fig. 1

Oxidizing equipment.

It was found that above 980°C, the copper sheet had a tendency to collapse, thus producing bent samples. It was then decided to cut the vacuum system at this temperature, and let a few cm^3 of air enter the tube. This process formed a very thin layer of cuprous oxide on the surface of the copper. Since cuprous oxide is much more refractory than copper, this thin layer was sufficient to prevent the copper from collapsing. After the sample had reached 1030°C, the temperature control was locked and the tube was opened to air. It was found that, at 1030°C, 1 1/2 hour was necessary to oxidize the copper completely. The temperature control was then turned up to 1090°C and the sample was annealed for two days in air, and for two more days under the relatively low vacuum provided by the fore-pump. The "charcoal-trap" vacuum was then established in the tube, the oven was turned off and the sample was allowed to cool down over a period of twelve hours.

The lengthy annealing process in air is to allow the formation of large single crystals from the originally formed polycrystalline material. The annealing under low vacuum is to remove from the cuprous oxide slab, any trace of cupric oxide or excess oxygen. The method employed to grow single crystals is a variation of the method used by Toth, Kilkson and Trivich (1960). Single crystals obtained by this method come out in slabs of about 1.5 x 1 x 0.015 cm, are transparent to red light, and their smooth surface needs no etching.

X-ray studies were performed on those crystals with a Norelco diffraction machine. The analysis was performed with the white radiation from a molybdenum tube operated at 50 KV, giving clear and sharp Laue transmission photographs on a blue medical Kodak film. Those photographs showed that:

1. samples are single crystals;
2. there is no trace of grain boundary, distortion, asterism or any other structural imperfection.

To find the orientation of a typical crystal, the points from the Laue pattern were plotted on a stereographic projection, using a Leonhardt chart and a Wulf net (Cullity 1956). The crystals were found to be oriented along the 3,1,1 plane. It is interesting to note that this orientation agrees with the one found by Kilkson and Trivich (1960) on their samples.

B. Apparatus for Photoconductivity

1. Equipment

a.) Sample Holder and Vacuum System

For the purpose of this experiment, the sample had to be subjected to a wide range of temperatures, from above 300°C down to liquid nitrogen temperature, without being exposed to air. Since electrical measurements had to be made at various temperatures, the holder had to be a good heat conductor, and yet, the sample had to be highly insulated from it. Besides, neither organic compounds nor alloys with discernable vapour pressure at 300°C could be used in the vicinity of the sample, for the latter adds some impurities to the sample, while the former reduces cuprous oxide at high temperatures. Finally, the holder had to be shielded against pick-up noises, for it was expected that the sample resistance might go as high as many thousands megohms. With those restrictions in mind, we arrived at the arrangement shown in Fig. 2.

A solid cylinder of oxygen free high-conductivity copper, five inches in length, half an inch in diameter, was truncated at one of its ends, and a slice was partially cut as shown in fig. 2A. A thin sheet of mica, cut into the proper shape, was inserted into the slit, and, by means of screws, fixed between the mica-insulated copper slices. This arrange-

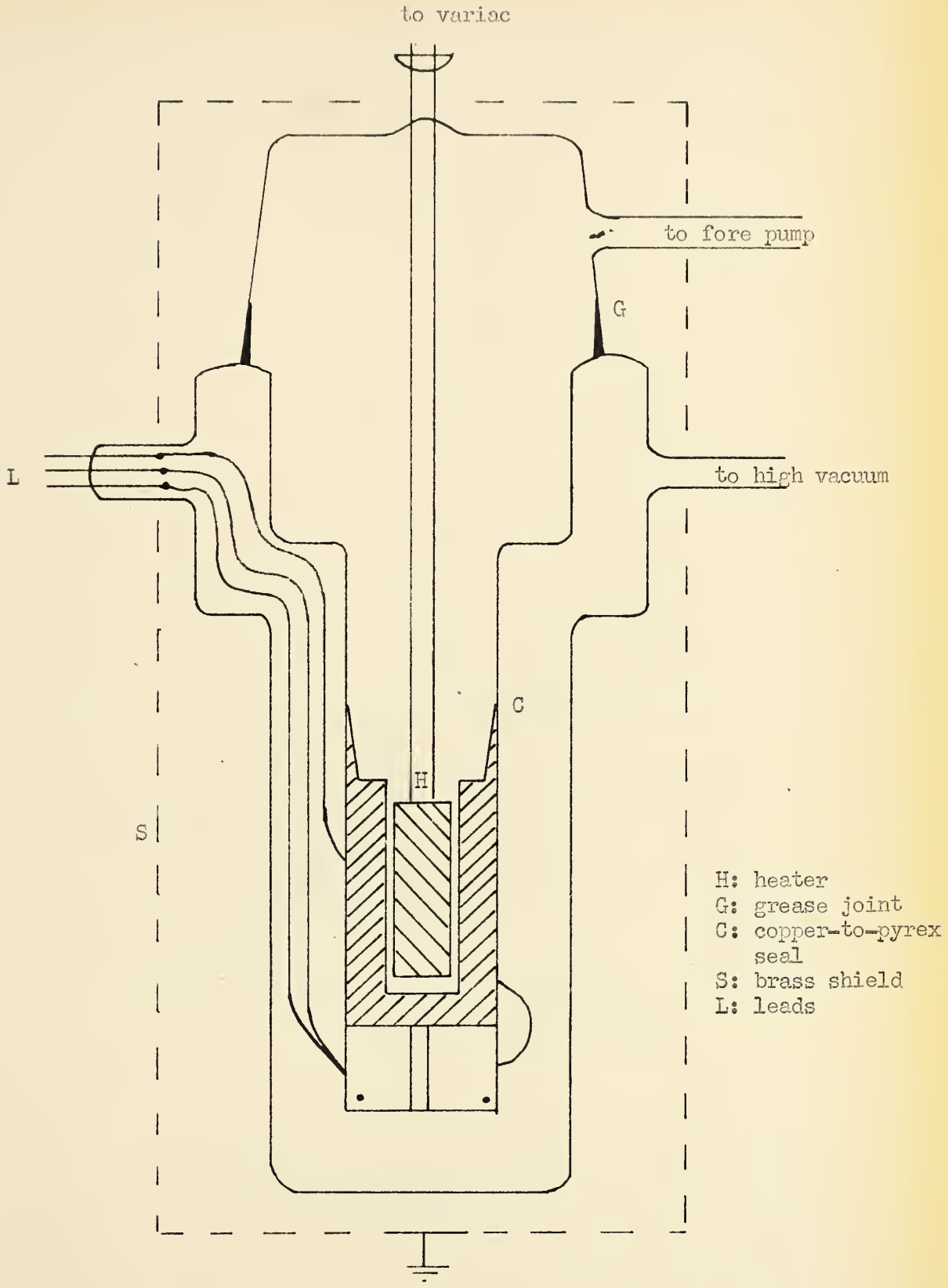

Fig. 2 - Sample Holder.

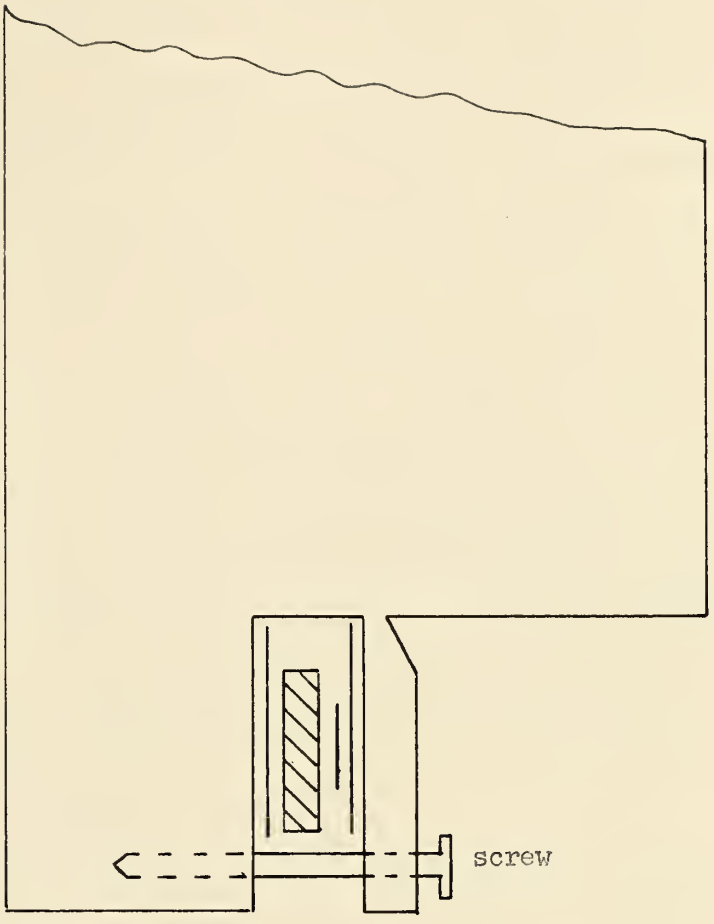

From left to right: copper-mica-sample-electrodes-mica-copper.

Fig. 2A - Vicinity of the sample.
(side view)

ment provided for the sample sufficient thermal contact with the main copper rod, as well as high insulation from it (about 10^{15} ohms).

Ohmic electrical contacts were provided by the insertion, between mica and sample, of two tiny rectangular pieces of platinum sheet. Leads for thermal and electrical measurements were spot-welded at the outer end of the platinum.

The upper end of the copper rod was drilled to a depth of 4 inches and a diameter of 3/8 of an inch. A 85-watt Chromalox pencil heater was inserted in the hole, to enable high temperature measurements. A Martin copper-to-pyrex seal was then hard soldered to the upper part of the copper cylinder. It was found that silver-copper eutectic (72% silver, 28% copper; melting point: 779°C), besides being vacuum tight, did not tend to deposit impurities on the sample at high temperatures, as did compounds containing cadmium or zinc in early trials.

The whole assembly, together with its vacuum jacket, is shown in Fig. 2. The auxiliary vacuum provided inside the dewar cup and around the heater was used at high temperatures to prevent slow oxidation of the copper walls. With this arrangement, a vacuum of better than 10^{-5} mm Hg could be obtained at the highest temperature, and better than 10^{-7} mm Hg at the lowest. Pressure was read on a Martin cold cathode vacuum gauge.

Finally, the sample holder and its vacuum jacket were put inside a grounded brass container for the purpose of shielding.

b.) Optical Equipment

As a light source, we used a Rival 355 42-watt tungsten bulb, fed by a 12-volt battery in parallel with a Heathkit battery charger. The steady voltage from the battery and the adjustment of the current at 3.5 amperes by means of a carbon rheostat, permitted a very steady light output. The light beam was focussed, by means of two cylindrical mirrors, on the entrance slit of a Leiss double monochromator. Analyzed by two prisms in series, the light came out of the exit slit with a spectral purity of about 3%, depending on the wavelength and on the slit width. The output of the monochromator, lying in the range .4 to 1.5 microns, was then focussed on the sample.

For A.C. measurements, the light beam was chopped at 37.9 cps with a mechanical sector; the sector was driven by a synchronous motor fed by a stabilized oscillator. Chopping frequency could be varied from about 5 cps up to 5,000 cps, ~~by~~ either by using a sector with different geometry, or by varying the frequency of the oscillator.

c.) Electrical Equipment

Bridge arrangement

The usual circuit used for photoconductivity measurements is as shown in Fig. 3. A known resistor is connected in series with the sample, and a D.C. supply is connected across the two, the photo-signal being read across the known resistor. Such an experimental set up was not satifactory for our purposes, because it introduces a D.C. component as well as the A.C. signal. Our high input impedance pre-amplifier -- to be described below -- could not accommodate any appreciable D.C. component without having its characteristics altered. We thus decided for the bridge arrangement shown in Fig. 4.

In this arrangement, the sample R becomes one arm of a bridge. The bridge is completed by a resistor R_1 of the same order of magnitude as R, and by a 100K Helipot potentiometer (R_2 and R_3). The bridge is fed by a 67 1/2 volt battery. With voltage on, and no signal, the helipot is adjusted until the center points of the bridge are equipotential. Then, locking the potentiometer in this position, light is shone onto the sample. R will change, causing an unbalance on the bridge. The signal obtained in this manner can be analyzed as follows.

With reference to Fig. 4, let $(V_1 - V_2)$ be the voltage

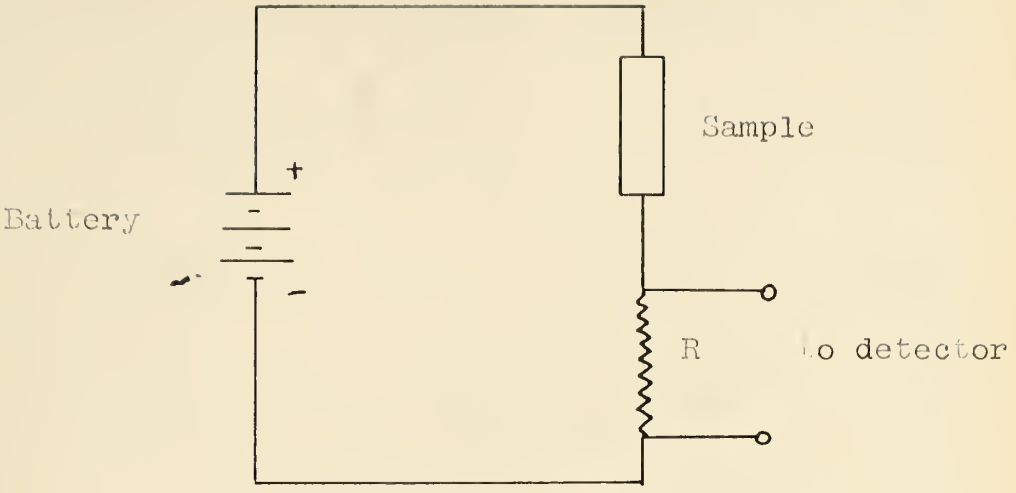

Fig. 3

Standard circuit for
Photoconductivity measurements.

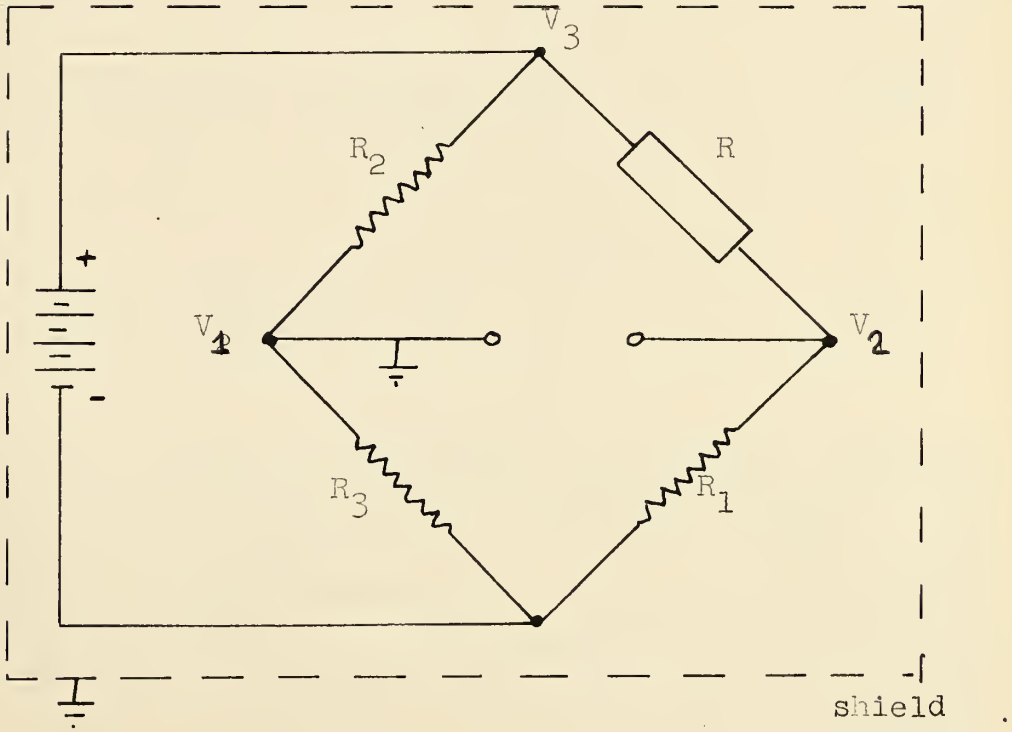

Fig. 4

Bridge Arrangement

across the center arms of the bridge. V_3 is the voltage of the battery. We have:

$$V_1 = \frac{R_3}{R_2 + R_3} V_3 \qquad (1)$$

$$V_2 = \frac{R_1}{R + R_1} V_3 \qquad (2)$$

$$V_1 - V_2 = V_3 \left(\frac{R_3}{R_2 + R_3} - \frac{R_1}{R + R_1}\right) \qquad (3)$$

$$\frac{d(V_1 - V_2)}{dR} = -V_3 \frac{R_1}{(R + R_1)^2}, \qquad (4)$$

independent of R_2 and R_3. At equilibrium, $V_2 - V_1 = 0$. Let dV be the signal across the center arms of the bridge, when there is an unbalance caused by a variation dR in R. From (4):

$$dV = -V_3 \frac{R_1}{(R + R_1)^2} dR \qquad (5)$$

and finally:

$$dR = \frac{(R + R_1)^2}{V_3 R_1} dV \qquad (6)$$

From equ. (6), the photocurrent can be calculated. From equ. (5), we see that dV depends on R_1, the known resistor. Maximizing dV with respect to R_1:

$$\frac{\delta(dV)}{\delta R_1} = -V_3 \frac{(R + R_1)^2 - 2R_1 (R+R_1) dR}{(R+R_1)^4} \qquad (7)$$

$$= 0, \text{ for } R = R_1$$

We thus obtain a maximum signal for this last condition. However, it was not always found practical to use a R_1 of the same size as R. This can be corrected for in the following manner. Putting $R_1 = R$ in (5) yields:

$$(dV) \text{ max.} = -V_3 \frac{1}{4R} dR \qquad (8)$$

Therefore, a plot of $\frac{R_1}{(R_1 + R)^2} / \frac{1}{4R}$ vs R_1/R could be used for signal amplitude corrections. Such a plot is shown in Fig. 5.

The function, of course, has a maximum of one for $R = R_1$. From the graph, it becomes obvious that the ratio R_1/R should always be kept as close to one as possible. However, when this is not possible, a correction factor for the signal amplitude can be found by taking the reciprocal of the ordinate corresponding to the value of R_1/R.

Besides satisfying the input requirements of our preamplifier, this bridge arrangement proved to be very versatile and useful, mainly for the following purposes:

1. it could be readily used for sensitive D.C. measurements in connection with a galvanometer amplifier or a D.C. electrometer;

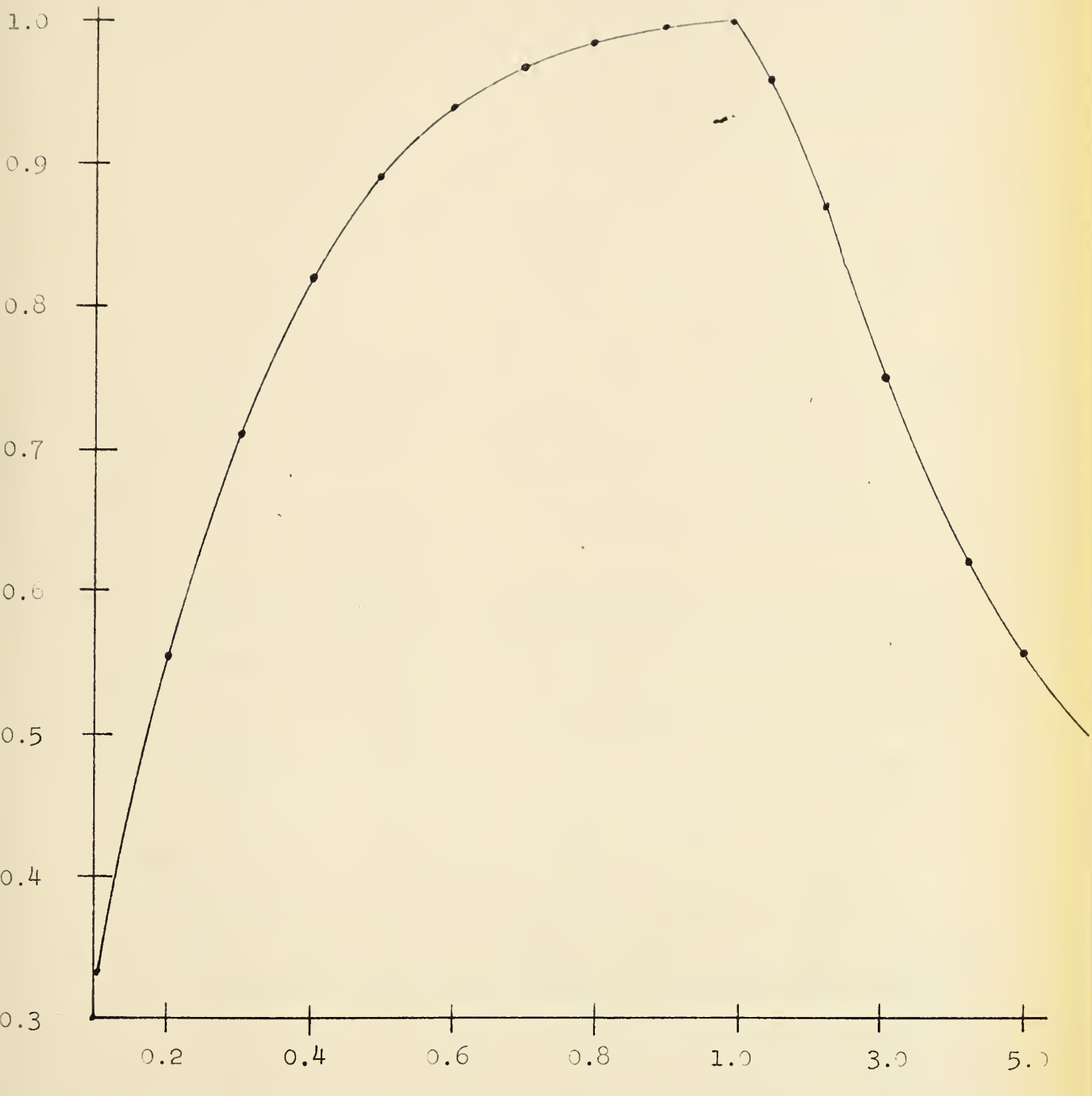

Fig. 5

Calibration of the bridge.

2. accurate measurements of resistivity vs temperature could easily be made;
3. when the sample resistance exceeded the limits of the input impedance of the preamplifier, a smaller R_1 resistor could be used, lowering the overall input impedance within reasonable limits;
4. finally, with reference to Fig. 5, it is seen that the bridge can be used as an "attenuator", by simply making $R_1/R \neq 1$, should the signal become strong enough to cause saturation in the preamplifier.

It should also be mentioned that all parts of the bridge were doubly shielded against stray A.C. signals.

Preamplifier

The main purpose of the preamplifier was to bring the high input impedance down to a value of about 10^6 ohms. The signal from the bridge is carried through a doubly shielded heavy coaxial cable to the grid of a CK 512AX electrometer tube. This stage is built inside a hole drilled in a heavy piece of brass. To achieve maximum stability, the preamplifier has its own B^+ and filament supply provided by batteries. There are two feedback loops: the first one feeds a D.C. voltage proportional to the input signal back to the

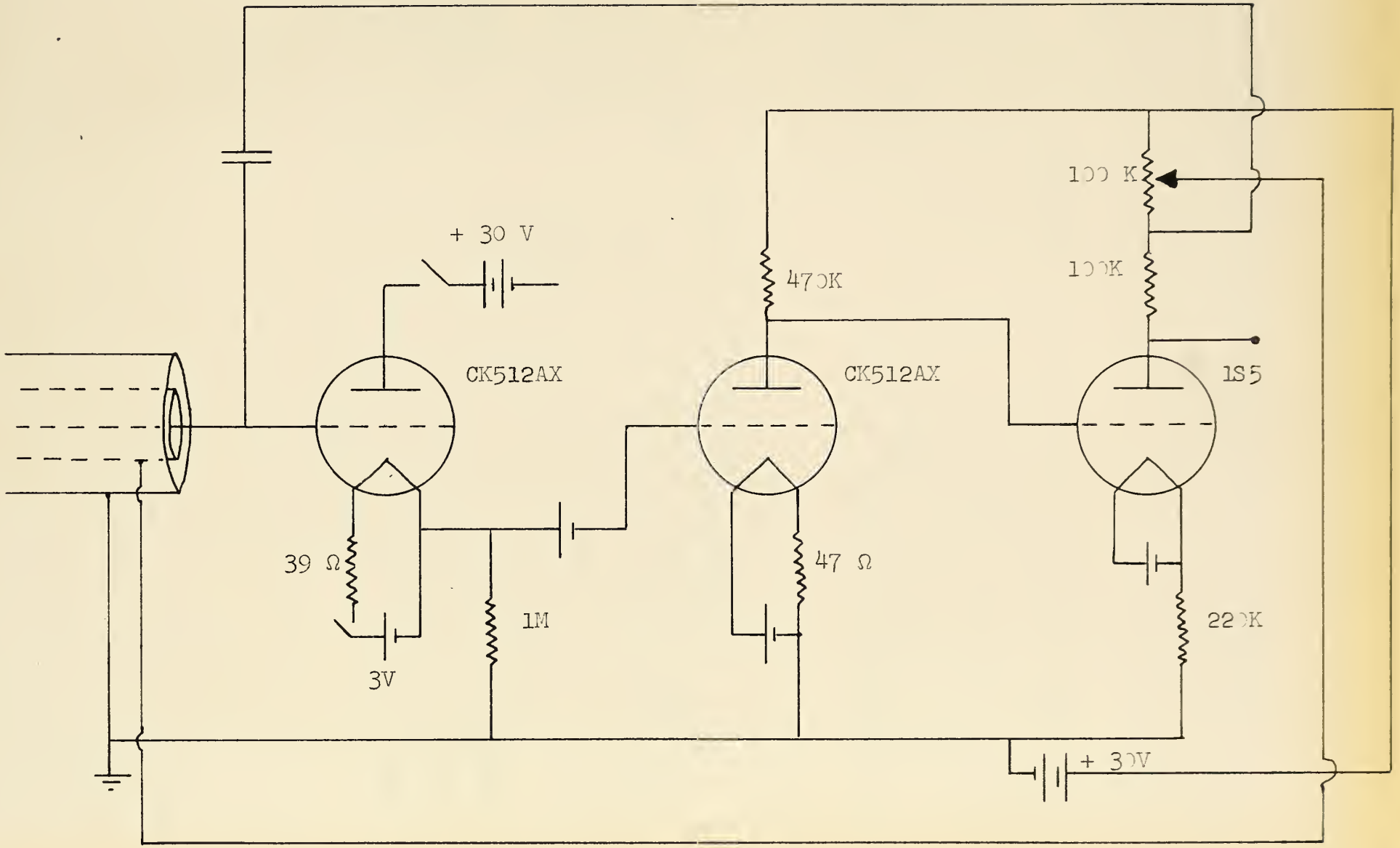

Fig. 6
Preamplifier

first shield, cancelling out the effect of any stray capacitance between the layers of the coax cable; the second one feeds an A.C. voltage back to the grid of the electrometer tube.

The preamplifier was submitted to intensive tests, before the actual experiment. It was found to be linear from 100 cps down to D.C., and it introduced no distortion at an input impedance of up to 100 megohms. Its amplification factor was about 4. A schematic diagram of the preamplifier is shown in Fig. c.

Amplifier and auxiliary equipment

The amplifier was a standard A.C. amplifier tuned at 37.9 cps. A by-pass switch, cutting the tuned circuit off, permitted the analysis of the square wave.

We used a Hewlett-Packard vacuum tube voltmeter to measure the synchronized output of the amplifier. Whenever examination of the wave shape was necessary (time constants measurements), a 536 Tektronix oscilloscope was used, together with a C-12 Tektronix oscilloscope camera.

2. Experimental Procedure

a.) R vs 1/T measurements

Before any photoconductivity measurements, we usually took a series of readings of the resistivity of our samples vs 1/T. For this purpose, we used either the bridge arrangement or a simple Avometer for resistance measurements, and a copper-constantan thermocouple together with a Leeds and Northrup portable potentiometer for temperature measurements. At low temperatures, when the resistance of the sample became too high, we used a Radiometer-Copenhagen megohmeter ($1 - 10^{8}$ Megohms) for resistance measurements.

b.) Source calibration

Since the energy output of our light source was not constant across the spectrum, the source had to be calibrated. This was done with the help of a Golay infra-red detector together with its electronic assembly: chopper and synchronous amplifier. The calibration curve could then be used to calculate correction factors for constant energy output at any wavelength. All our photoconductivity measurements have been corrected for constant energy illumination.

c.) Photoconductivity

Experiments have been performed on two kinds of crystals: mosaic[+] structure crystals with grain size of about 1 mm^3, and single crystals. Procedure was the same for both. They were slowly heated in the holder, up to 100°C, and left for a few days, under high vacuum (better than 10^{-6} mm Hg). Photoconductivity measurements were taken at 90°C, 22°C, -50°C and -125°C. Temperatures below room temperature were obtained with refrigerant baths: solid carbon dioxide and methyl alcohol, or liquid air. In all cases, temperature remained constant within ± 0.5°C throughout the experiment.

[+] By mosaic crystal, we mean a sample formed of large crystallites, separated by sharp boundaries. (A good analogy of that structure would be a floor tile; for pictures of mosaic crystals, see Blankenburg -1952-.)

III. PHOTOCONDUCTIVITY

INTRODUCTION

Photoconductivity in cuprous oxide, as in other materials, is not easily interpreted. This phenomenon is best understood in relation with other properties of the material, like its optical transmission and conductivity vs temperature characteristics. Since optical transmission studies are beyond the scope of the present work, we will have to rely heavily on investigations made by previous authors on this particular aspect.

Our equipment, however, could easily and quickly give the conductivity vs temperature characteristics of the samples. In order to gain more information about our crystals, we then performed for each of them an experimental determination of the conductivity curves. The first part of this chapter will deal with this particular aspect.

In the second part, the theory of photoconductivity is examined. The third part contains a critical survey of the literature on the subject, up to the present day, while in the fourth part, we present our own results. Finally, the chapter is closed by an interpretation of those results.

A. CONDUCTIVITY

The equipment used for conductivity measurements has been described in the preceding chapter, so that nothing will be said about it here. Instead, we start by a few lines on the theory of conductivity. This will be followed by a brief survey of the literature, and the presentation and interpretation of our own results.

1. Theory

According to the band theory of solids, the permitted energy levels in solids can be represented by bands separated by gaps of forbidden energy. In the case of a semiconducting crystal (as for an insulator), the theory assumes that at absolute zero of temperature, all the allowed bands are either completely filled or completely empty, so that electrical conduction cannot occur. For a semiconductor, the width of the forbidden energy gap between the full valence band and the empty conduction band, is of the order of one electron-volt. Therefore, as the temperature is increased, electrons can be thermally excited from the valence band to the conduction band, leaving holes in the valence band; both electron and hole currents will then result upon application of an electric field across the sample. Besides this type of conductivity, named intrinsic conductivity, there can also exist extrinsic

conductivity. The latter stems from impurity atoms, whose energy levels are situated in the forbidden gap. Those impurities can be of the donor type, giving electrons to the conduction band (n-type conductivity), or acceptor type, giving holes to the valence band (p-type conductivity). Most semiconductors are of the extrinsic type at room temperature and lower.

The temperature dependence of conductivity in semiconductors has been shown to be of the form:

$$\sigma = A_1 e^{-\epsilon_1/kT} + A_2 e^{-\epsilon_2/kT} + \text{---} A_n e^{-\epsilon_n/kT} \qquad (A1)$$

where ϵ_1 is the "activation energy" for intrinsic conductivity, and ϵ_2 --- ϵ_n are the activation energies for extrinsic conductivity (corresponding to different impurity levels). Each of those terms will be dominant within a certain range of temperatures. Therefore, a plot of log σ vs 1/T yields straight lines whose slopes can be used to determine the band gap and the position of the impurity levels. In compound semiconductors, like cuprous oxide, impurities may come from a stoichiometric excess of one constituent. This, in conjunction with the well known fact that cuprous oxide is a p-type semiconductor, will be used later in connection with the interpretation of our results.

2. Survey of the literature

The electrical conductivity of cuprous oxide has been investigated by many authors. A few of their results will be indicated here.

The first conductivity measurements over a wide range of temperatures were made by Juse and Kurtschatov (1932). They found for ϵ_1 and ϵ_2 .72 ev and .13 ev respectively. The results were interpreted to mean that Cu_2O had a band gap of 1.44 ev, and an impurity level at .26 ev above the valence band, caused by the stoichiometric excess of oxygen. More recently, Anderson and Greenwood (1952), working on samples annealed at 1050°C in vacuo, found for ϵ_1 and ϵ_2, 1.04 and .30 ev respectively. It was noticed that samples exposed to 9 mm O_2 exhibited a lower activation energy in both ranges, of .844 and .238 ev respectively. Böttger (1952) investigated the dependence of the conductivity on the oxygen pressure at 900°C. He found that the conductivity of cuprous oxide was proportional to the 1/7th power of the oxygen pressure. When he plotted the activation energy versus pressure, he found a critical point at 10^{-3} mm Hg of pressure; the activation energy is about .6 ev just above this pressure, and remains constant at 1.0 ev below the same point. It is reasonable to assume that this last value is associated with the intrinsic range.

Of more immediate interest to the present work, are the measurements of Weichman (1960). Working on samples submitted to a similar outgassing process as in our case, and under similar experimental conditions, he finds for the intrinsic range, an activation energy of 1.0 ev. Moreover, an impurity level at .3 ev above the valence band is found to be responsible for conductivity between 350°C and 80°C.

All those investigations were made on polycrystalline material. Very recent measurements however have been made on single crystals. In a study at high temperatures, Toth, Kilkson and Trivich (1961) find an activation energy varying from .65 ev up to 1.05 ev, for oxygen pressures going from 10 mm Hg, down to 10^{-5} mm Hg. Performing a similar study, O'Keefe and Moore (1961) find that except at very low oxygen pressures, the conductivity at all temperatures is due entirely to positive holes associated with cation vacancies. In the intrinsic range, they find an activation energy of .98 ev.

3. Own results

Our own measurements were performed on two kinds of crystals: a polycrystalline sample of conductivity $\sigma = 5 \times 10^{-4}$ ohms^{-1} cm^{-1} at room temperature, and a single crystal of $\sigma = 5 \times 10^{-5}$ ohms^{-1} cm^{-1} at room temperature. Both were outgassed in vacuo at 1000°C before their in-

stallation in the holder. All measurements were taken at pressures below 10^{-4} mm Hg, as read on the gauge; in terms of oxygen pressure, this means at least an order of magnitude lower.+ Both polycrystalline sample and single crystal having been studied under the same experimental conditions, it should then be possible to determine whether or not the crystalline structure has a definite bearing on the activation energies.

Fig. 7 shows the conductivity curves for both crystals. From those curves, we calculated the values of the constants "A" and "ϵ" (see eq. A1).

For the single crystal, we find:

$A_2 = 9.7 \times \text{ohms}^{-1}\ \text{cm}^{-1}$; $\epsilon_2 = 0.52$ ev ($300^\circ C < T < -75^\circ C$)

$A_3 = 2.8 \times 10^{-11}\ \text{ohms}^{-1}\ \text{cm}^{-1}$; $\epsilon_3 = 0.026$ ev ($-75^\circ C < T < -125^\circ C$)

For the mosaic crystal:

$A_1 = .88 \times 10^{5}\ \text{ohms}^{-1}\ \text{cm}^{-1}$; $\epsilon_1 = 1.0$ ev ($T > 300^\circ C$)

$A_2 = 7.2 \times \text{ohms}^{-1}\ \text{cm}^{-1}$; $\epsilon_2 = 0.40$ ev ($300^\circ C < T < -75^\circ C$)

$A_3 = 5.2 \times 10^{-10}\ \text{ohms}^{-1}\ \text{cm}^{-1}$; $\epsilon_3 = 0.026$ ev ($-75^\circ C < T < -125^\circ C$)

(Two other samples, a single crystal and a polycrystalline sample, were also studied with respect to their conductivities. Their respective values correspond closely to the values cited above.)

+ The gauge measure the gas pressure; above room temperature, besides nitrogen, we have present in the holder residual water vapour and other contaminations.

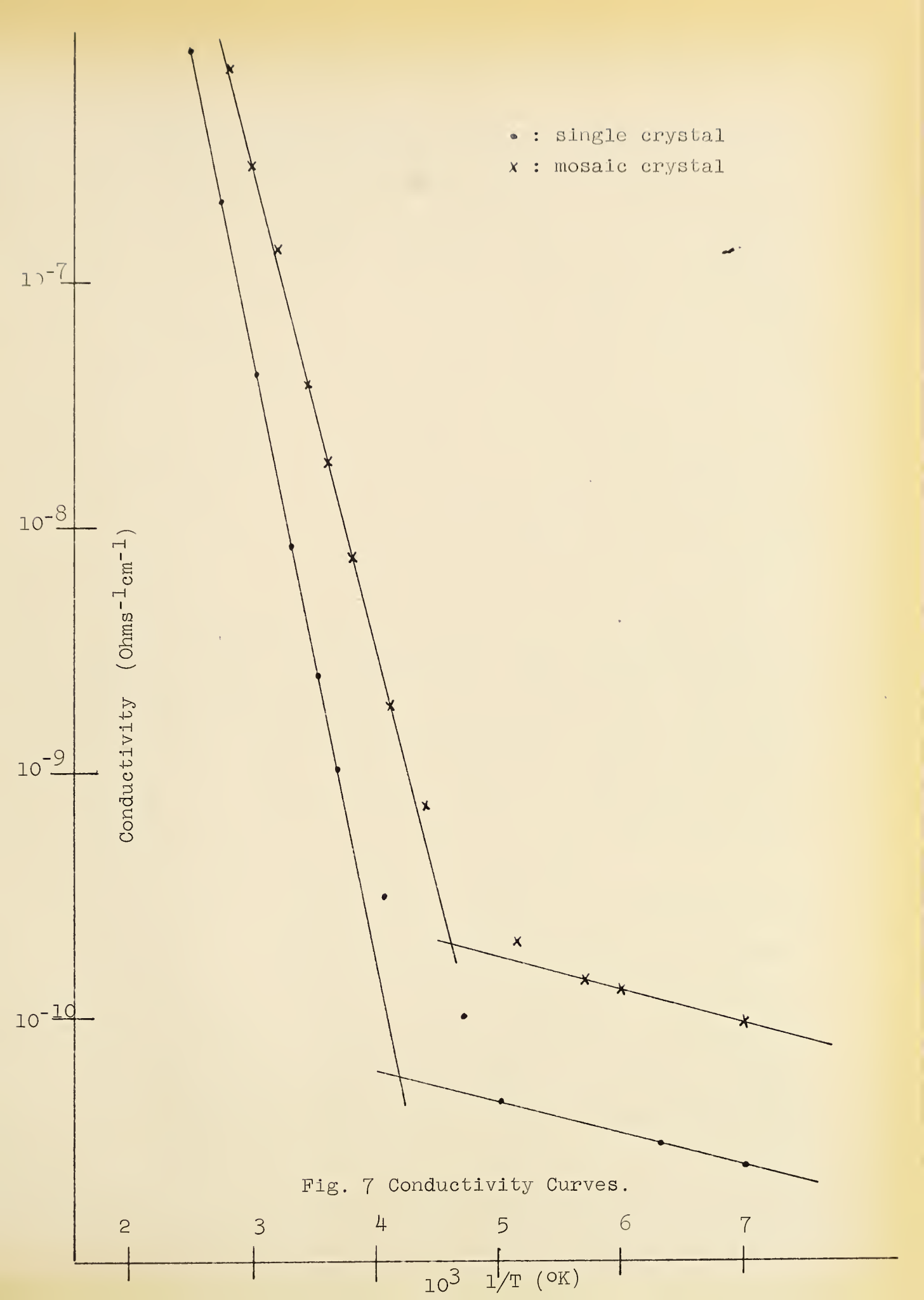

Fig. 7 Conductivity Curves.

For the single crystal, it was not possible to reach the intrinsic range temperature; however, measurements in the intrinsic range, made on other single crystals, which were not used for photoconductivity experiments, yielded the value of one ev for the activation energy in this range. We thus obtain a band gap of two ev for both types of crystals, agreeing closely with most previous authors. In view of that, it seems reasonable to conclude that the thermal band gap of cuprous oxide is independent of the structural perfection of the sample; rather, as was shown by the work of Toth and al. (1961), the band gap still depends strongly on the oxygen pressure.

The slopes of 0.51 ev and 0.40 ev in the range from 300°C to - 75°C are unmistakable. Most authors find an activation energy of about 0.3 ev in this range. However, calculations from the curves obtained by O'Keefe and Moore (1961), on single crystals, reveals that for measurements taken at a pressure of 10^{-5} mm of Hg, they also found 0.51 ev for the activation energy in this range.

We have to suggest, with Weichman and others, that this level is an acceptor level, due to excess oxygen or copper vacancies in the lattice: its exact position varies from sample to sample. However, from the results of O'Keefe and Moore and from our own results, there is a definite "trend" for the position of this level: it is situated higher above

the valence band when the resistivity of the sample is larger, and also when the experimental conditions are such that the Cu_2O contains less extra oxygen. Our mosaic crystal, for instance, had a resistivity ten times lower than the single crystal, and had been exposed to air at atmospheric pressure (at 300°C) for a few minutes before the conductivity measurements: consequently, we find the impurity level to lie at .2 ev below the corresponding level for the single crystal. There is also another possibility: the apparent position of this level may be changed by the presence of a donor level, being also effective in the same temperature range.* Bloem (1958) suggests the presence of such a level, and interprets it as being caused by copper excess in the lattice.

At lower temperatures, a slope of 0.026 ev was found for both crystals. However, there is a major correction to be considered here. According to Mott and Fröhlich (1939), the mobility in Cu_2O varies as:

$$\mu = \mu_o e^{\theta/T} \qquad (A2)$$

where T is the absolute temperature, and θ, the Debye temperature (about 300°K for cuprous oxide). Therefore, the conductivity varies as:

$$\sigma = ne\mu = eN_o\mu_o e^{\frac{K\theta - \epsilon}{KT}} \qquad (A3)$$

where n is the concentration of free carriers at any temper-

* $300^\circ C < T < -75^\circ C$

ature T, and N_o is a constant. For ϵ large, one can neglect the term $K\Theta$ in the exponential. At low temperatures however, it becomes important, and in our case here, the measured slope may be interpreted as $K\Theta - \epsilon$, and not ϵ alone. Since $K\Theta \simeq$ 0.025 ev, we get for the "corrected" ϵ, a value of 0.05 ev, or an acceptor level at 0.1 ev above the valence band. It must be noted however, that the analysis of Mott and Fröhlich is based on the assumption that Cu_2O is a polar semiconductor.

An exact interpretation of the conductivity of Cu_2O in the extrinsic range is still to come. Most investigators find the same "types" of impurity levels, but the position of those levels varies widely. The new methods of growing single crystals will presumably improve the reproducibility of the results. At the present time, it is not possible to decide whether or not the monocrystallinity of a sample has a definite bearing on the extrinsic activation energies.

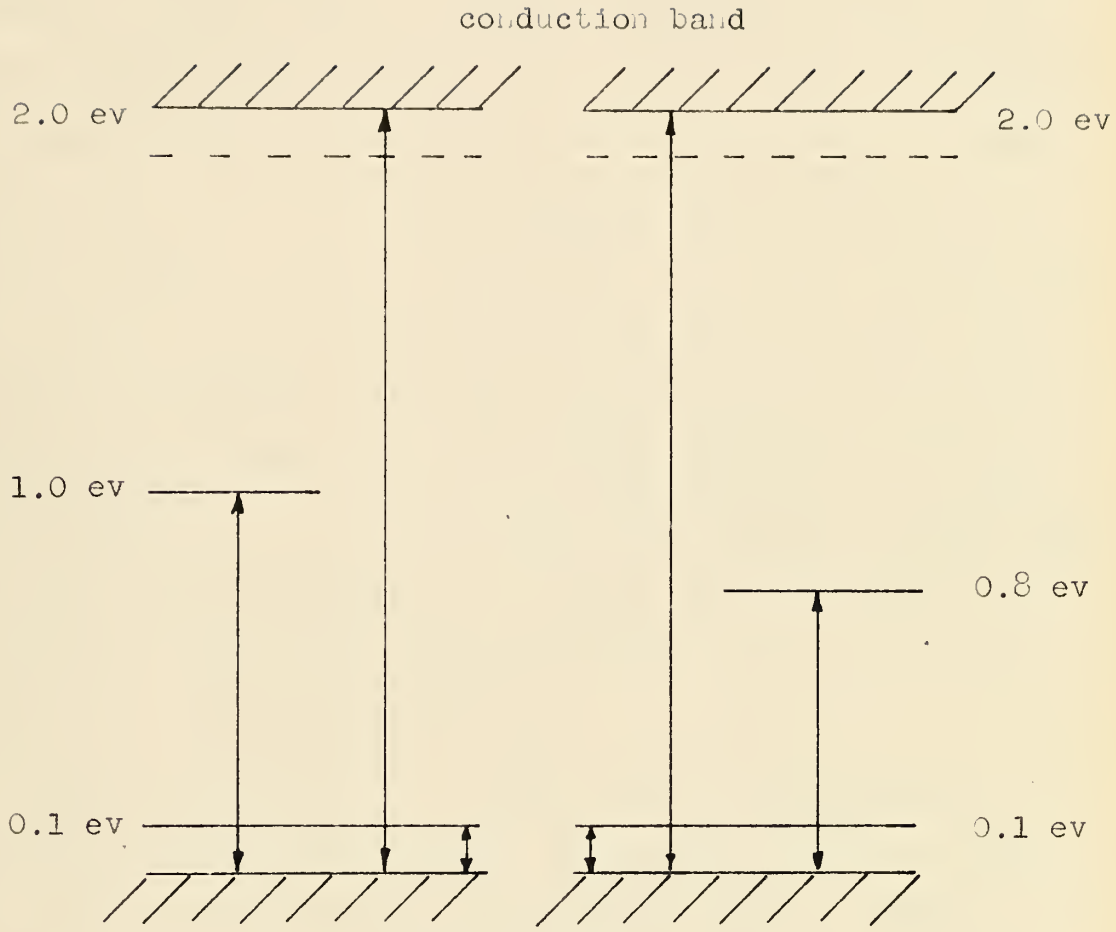

Fig. 8

Energy diagram from conductivity measurements --

Left: single crystal
Right: mosaic crystal

B. THEORY OF PHOTOCONDUCTIVITY

1. General

In the preceding section, we have seen that, according to the band model of a semiconductor, electrons can be thermally excited from the valence to the conduction band, leaving holes in the valence band. We have also considered the case where electrons can be thermally excited to bound states lying in the forbidden energy gap, giving positive charge carriers in the valence band. At a given temperature, since there is an equilibrium established between the rate of thermal excitation of charge carriers and their rate of recombination, there is a certain concentration of charge carriers present in both the conduction and the valence band. This gives rise to electrical current, upon application of an electric field. This type of conductivity can be referred to as "dark" conductivity.

Upon illumination of a sample with electromagnetic radiation of sufficient energy, it is also possible to excite current carriers into the conduction band. These optically excited carriers will also have a certain recombination probability, and an equilibrium will be established between the rate of creation of current carriers, and their rate of recombination. Therefore, at any given temperature, there will be present, over the concentration of charge

carriers thermally excited, an excess concentration of optically excited carriers, and of course, a corresponding increase in conductivity. Such an increase in conductivity upon illumination is called photoconductivity. As in the case of "dark" conductivity, one can have intrinsic photoconductivity, and extrinsic photoconductivity. The latter involves optical excitations to or from an impurity level lying in the forbidden energy gap, while the former occurs when the radiation has enough energy to create an electron-hole pair, by raising an electron from the valence band to the conduction band.

According to Rose (1954), the most general relation characterizing photoconductivity can be written as:

$$N = F\tau \qquad \text{(B1)}$$

where N is the steady state increase in the density of free carriers generated by L excitations per second in the sample, and τ is the lifetime of these carriers in the free states. Eq. (B1) also implies that in order to reach a steady state, the rate of disappearance of carriers must be equal to their rate of generation. The rate of disappearance of carriers is determined by their recombination into ground states, from which they have to be optically reexcited. Ground states should be carefully distinguished from shallow trapping states, from which the carriers can be thermally reexcited.

Equation (B1) can be converted into an extra conductivity through:

$$\sigma = Ne\mu \qquad (B2)$$

where the symbols have their usual meaning. It is then possible to compute the photocurrent, from the knowledge of σ, the size of a given specimen, and the applied voltage.

2. Spectral Dependence

For most photoconductors, the spectral sensitivity decreases exponentially with decreasing photon energy, in the region of the optical absorption edge. Starting from this fact, Moss (1952) has shown that one can determine from the spectral sensitivity of a photoconductor, the "threshold" wavelength, from which the optical activation energy can be determined for comparison with the optical absorption or conductivity measurements.

For this purpose, he considers a monatomic solid, therefore an intrinsic semiconductor, in which the thermal and optical activation energies should be the same.

, The spectral sensitivity curve is represented by:

$$S(E) = \left[1 + \exp\ \beta(E-E_o)\right]^{-1} \qquad (B3)$$

where β is a constant, E is the energy at any wavelength, and E_o the energy at the "threshold" wavelength. This curve

exhibits a flat response at short wavelengths, ($E \gg E_o$) and an exponential fall with energy at long wavelengths. Moss assumes that such a sensitivity variation results from the distribution of energy levels from which the photoelectrons originate (or, alternatively, to which they may go).

If the distribution is such that there are $N(E)\,dE$ levels between E and $E + dE$, then, with a radiation of a given quantum of energy E_λ, the amount of absorption, and hence the sensitivity, will be proportional to the total number of centers of energy lower than E_λ. Hence:

$$S(E) \quad \alpha \quad \int_0^{E_\lambda} N(E)dE \qquad (B4)$$

or

$$N(E) = G \quad \frac{d \quad S(E)}{dE} \qquad (B5)$$

where G is a constant. Using the expression for S(E):

$$N(E) = \frac{G\beta \exp\left[\beta(E_o - E)\right]}{\left[1 + \exp \quad \beta(E_o - E)\right]^2} \qquad (Bo)$$

From this expression for the distribution of levels, the number of electrons which will be present in the conduction band due to thermal excitation can be calculated. If one takes the zero of energy at the bottom of the conduction band, the number of electrons raised thermally to the conduction band is given by:

$$C \left\{ N(E) \right\}^{1/2} \exp(-E/2kT)dE \qquad (B7)$$

where C is a constant. The total number will therefore be:

$$n = C \int \left\{ N(E) \right\}^{1/2} \exp(-E/2kT)dE \qquad (B8)$$

Substituting for $N(E)$ and putting $\Phi = E - E_o$, one obtains:

$$n = C(G\beta)^{1/2} \int \frac{\exp(\beta\Phi/2) \exp(\Phi - E_o)/2kT}{1 + \exp(\beta\Phi)} d\Phi \qquad (B9)$$

where the limits of integration should be taken from the bottom to the top of the valence band. if $\beta >> 1/kT$, the limits $-\infty$ to $+\infty$ can be used as an excellent approximation. On rearranging the terms, the integral becomes:

$$n = C(G\beta)^{1/2} \int_{-\infty}^{\infty} \frac{\exp\left[1/2\Phi\left\{\beta + (1/kT)\right\}\right] \exp(-E_o/2kT)}{1 + \exp(\beta\Phi)} d\Phi \qquad (B10)$$

$$= C\left(\frac{G}{\beta}\right)^{1/2} \frac{\pi}{\sin\pi a} \exp(-E_o/2kT)$$

where $2a = 1 + 1/\beta kT$. It is immediately seen that this expression has the same form as:

$$n = n_o e^{-w/2kT}$$

the expression occuring in the conductivity theory. By comparison, $W = E_o$, and therefore, when $E = W$, the sensitivity becomes:

$$S = \left[1 + \exp\left\{ \beta(E_o - E_o) \right\} \right]^{-1} = 1/2 \qquad (B11)$$

We thus reach the important conclusion that it is possible to determine the activation energy from the point on the photoconductivity curve where the sensitivity has fallen to half its maximum value: activation energy = quantum energy at $\lambda_{1/2}$. Moss extends this argument by saying that in the case where two or more bands of sensitivity are present, the activation energy of the longer wavelengths bands will be determined from the wavelength where the sensitivity has fallen to half its value, with respect to the flat part of the curve immediately preceding the exponential fall. In other words, this conclusion can also be applied to impurity photoconductors.

In practice however, it is seen that the flat section of the spectral sensitivity curve, as predicted by Moss for wavelengths shorter than the absorption edge, does not exist, Instead, the usual photoconductivity measurements show a peaked curve, with a maximum close to the optical absorption edge. The decay, around the absorption edge however, follows closely an exponential law.

To explain the peaked response curve, we must first consider the change of behaviour of the crystal with respect to the incident light as we pass from the long wave to the short wave side of the absorption edge. As we go from longer to shorter wavelengths, we pass from a small value of the absorption coefficient to an extremely large value; therefore, al-

though the longer wavelengths will be absorbed to some extent throughout the crystal, the shorter wavelengths will be effective only in a very small thin outer layer. Experimentally, it is found that except for measurements on very thin layers, the sensitivity drops rapidly with increasing absorption coefficient. Two explanations have been given to account for this.

Gudden and Pohl (1923) suggested that the photodissociation of an electron-hole pair might be impossible for direct valence-to-conduction band transitions, being only possible at an impurity center. According to this hypothesis, the absorption of light beyond the absorption edge should only cause heating.

Rose (1951) has given a different explanation. Since the absorption coefficient is very high on the short wavelength side of the absorption edge, the photoconductive transitions occur in a very thin layer. The extremely small photocurrents observed are then due to space charge limitations, similar to the case of the vacuum diode. According to Rose, the effects are about seven orders of magnitude greater in a photoconductor than in a diode. Furthermore, the higher density of carriers in these thin layers will result in a greater recombination probability, thus reducing the average lifetime of a carrier in the free states, and consequently, the photoconductivity. Thus, for spectral regions where the absorption coefficient is of the order of 10^{+5} cm^{-1}, samples of thickness

of the order of one micron should be used; in that case, the spectral response curve assumed by Moss in the derivation of the activation energy should be justified. This has been verified experimentally several times; Moss (1949) for instance, has observed a fairly flat response, followed by an exponential fall over a range of 10, 000 : 1 on lead sulphide layers.

3. Temperature Dependence

Photocurrents have been observed both to increase and to decrease with temperature. If for instance we consider an expression for the lifetime of a free carrier as $\tau = 1/vsn$, where v is the thermal velocity, s the capture cross-section of a capturing center, and n is the number of these centers, we see that v will increase with temperature, decreasing τ, and, consequently, decreasing the sensitivity. On the other hand, the capture cross-section might decrease faster than v increases, and in such a case, one would expect a greater sensitivity at higher temperatures. In general, the interpretation of the temperature dependence of photocurrents is hazardous, because more than one parameter can change with temperature. A semi-quantitative argument will be given in the section dealing with traps.

On the other hand, while the theoretical study of the magnitude of the photocurrent vs temperature presents some

difficulty, the behaviour of the spectral sensitivity, under temperature variations, can be readily predicted. In general, the spectral sensitivity curve can be expected to shift towards shorter wavelengths, as the temperature is decreased. We have seen in the previous section, that it was possible to relate the optical absorption edge to the $\lambda_{1/2}$ value of the photoconductivity curve. Thus, the shift of the spectral sensitivity curve is a direct consequence of the shift towards shorter wavelengths, experienced by the optical absorption edge, as one goes down in temperature. This effect is believed to be due to:

(a) the variation of the bandwidths with temperature;

(b) the relative movement of the energy bands, as the temperature is altered, with a resulting lowering or increasing of the forbidden gap.

The two effects are extensively discussed by Fan (1951) and by Bardeen and Shockley (1950). They find the shift to be linear with temperature. In most semiconductors, it is of the order of magnitude of 10^{-4} ev/°C.

4. Trapping -- Time constants -- Quantum efficiency

These three subjects have been put under a same heading, because they are all interdependent; they will be first of all shortly treated separately. Then, an equation for the photo-

current, including trapping effects and transient responses, will be derived.

a.) Trapping

A trap is an impurity or crystal defect level, situated in the forbidden energy gap, near the band edges, and capable of holding carriers of one sign for a certain amount of time. One can speak of shallow traps, or of deep traps, depending on whether they are close or far from their respective band edges. By definition, recombination will not take place to a large extent at a trapping level, but rather, the carriers will be thermally reexcited into their respective bands, before they can recombine. Since the trapping process involves thermal reexcitation, it will become noticeable at lower temperatures, when the carriers spend a significant amount of time in the traps before being reexcited.

b.) Time constants

Trapping will affect the time required to set up the steady-state photocurrent and the time required for these photocurrents to decay when the optical excitation is interrupted. The rise time is increased, because in order to increase the density of free carriers, the density of carriers in the shallow trapping states has to be increased in the same

proportion. The rise time is thus increased by ratio of shallow-trapped to free carriers. Similarly, when the optical excitation is interrupted, the shallow-trapped carriers must be emptied into the ground states via the free states. The observed rise time, or decay time of the photocurrent, is thus not necessarily the same as the lifetime of a free carrier. Since at lower temperatures the thermal reexcitation of trapped carriers is slower, the equilibrium between the number of carriers being trapped and the number being reexcited, will ~~be~~ take longer to establish, thus increasing the observed rise and decay times.

c.) Quantum efficiency

In the earlier work on photoconductivity, much consideration was given to the distinction between primary photocurrents, and secondary photocurrents. Among the characteristic distinctions between the two effects, were the following. The primary currents are "instantaneous", in comparison with the appreciable time lag of the secondary currents. The measured primary currents are proportional to the applied field for small fields, with saturation at high fields, as compared to the more complicated field dependence of the secondary currents. Further differences are the small temperature dependence of the primary currents, as compared to the marked

temperature dependence of the secondary currents, and the proportionality to light intensity of the former, compared to the hysteresis effects of the latter. Furthermore, there is a maximum "quantum efficiency" of unity in the primary currents, and a possible greater efficiency in the secondary currents. In the light of what we have seen before, on traping and time constants, these distinctions can be summed as follows: the primary photocurrent is the one for which traping is absent or negligible, while in the case of the secondary currents, trapping becomes important.

We have introduced the term "quantum efficiency", and in order to illustrate what is meant by that, let us assume a p-type semiconductor with some deep traps. By "deep", we mean that the traps are able to hold the electron for a considerable length of time, before thermal reexcitation in the conduction band, and eventual recombination. While the electron is trapped, the hole that is left behind in the valence band will be able to move towards the negative electrode. When the hole reaches the electrode, one charge will have reached the electrode for the single photon; thus, a quantum efficiency of one has been achieved. However, we have assumed a deep trap; thus, at this time, the electron is still in its impurity level, and consequently, when the hole combines with an electron at the cathode, the crystal will become negatively charged. So,

an extra negative charge will be given off at the anode,

creating another hole. If this hole too can reach the cathode before recombination takes place, a quantum efficiency of two will appear to exist. In general, the apparent quantum efficiency will be given by $G = \frac{\tau}{\tau_r}$, where τ is the average time spent by the electron in the trap, and τ_r the transit time of the hole between the electrodes. Rose (1954) has introduced the term "gain" for G, reserving the name "quantum efficiency" for primary processes, i.e. the ratio of excitations to incident photons.

5. Simple photoconductivity equation, including trapping and transient effects

We will assume a hole photoconductor, with a single set of electron traps, situated a few kT below the conduction band. The temperature is supposed to be low enough, so that the dark conductivity of the sample can be neglected; also, recombination does not occur in the traps. We further assume that the applied electric field is low, so that the concentrations of photo-carriers are independent of the position, and therefore, are a direct measure of the photocurrents. Under those conditions, we define the following terms:

L: number of optical excitations per unit volume per unit time;

R: electron-hole recombination coefficient;

N: number of electron traps per unit volume;

n_e: electron concentration in the conduction band;

n_h: hole concentration in the valence band;

Tn_eN: rate of electron trapping;

n_t: electron concentration in the traps;

En_t: rate of thermal evaporation of the trapped carriers back into the conducting band.

The rate equations are then:

$$\frac{dn_t}{dt} = Tn_eN - En_t \qquad \text{(B12)}$$

$$\frac{dn_e}{dt} = L - Tn_eN - Rn_en_h + En_t \qquad \text{(B13)}$$

$$\frac{dn_h}{dt} = L - Rn_en_h \qquad \text{(B14)}$$

We eventually want n_h as a function of t. We can immediately see that those three equations are in reality equivalent to two, since (B13) is a linear combination of (B12) and (B14). This comes from the fact that $n_h = n_e + n_t$. Rearranging the equations, one now gets:

$$\frac{dn_t}{dt} = Tn_eN - En_t \qquad \text{(B15)}$$

$$\frac{d(n_t + n_e)}{dt} = L - Rn_e\,(n_e + n_t) \qquad \text{(B16)}$$

The steady-state solution is obtained by setting both derivatives equal to zero:

$$n_{e_o} = \left[\frac{L}{R}\left(1 + \frac{TN}{E}\right)^{-1}\right]^{1/2} \qquad (B17)$$

$$n_{t_o} = \frac{TN}{E}\left[\frac{L}{R}\left(1 + \frac{TN}{E}\right)^{-1}\right]^{1/2} \qquad (B18)$$

and

$$n_{h_o} = n_{e_o} + n_{t_o} = \left[\frac{L}{R}\left(1+\frac{TN}{E}\right)\right]^{1/2} \qquad (B19)$$

(In the absence of traps ($N = 0$), $n_o = (L/R)^{1/2}$, the well-known one-half power dependence of photoconductivity on illumination at high level; $n_{t_o} = 0$, of course, and $n_{e_o} = n_{h_o}$.)

In order to get an approximate value of the decay time constant, let $\alpha = n_e/n_t \simeq n_{e_o}/n_{t_o} = E/TN$ and let the light source be interrrupted ($L = 0$); then, using (B16):

$$\frac{d(n_e + n_t)}{dt} = \frac{dn_h}{dt} = -Rn_e(n_e + n_t) \qquad (B20)$$

or:

$$(\alpha + 1)\ \frac{dn_t}{dt} = \frac{dn_h}{dt} = -R\alpha n_t^{\,2}\ (\alpha + 1) \qquad (B21)$$

Thus, assuming that the time constants involved in thermal re-excitation are long as compared to recombination constants:

$$\frac{dn_h}{dt} = \frac{dn_t}{dt} = -R\alpha n_t^{\,2} \qquad (B22)$$

therefore

$$n_t \simeq n_h = n_{h_o}(1 + n_{h_o} R\alpha t)^{-1} \qquad (B23)$$

The time constant is therefore of the order of:

$$t \simeq \frac{1}{\alpha R n_{t_o}} \simeq \frac{1}{R n_{e_o}} \simeq \left[\frac{1 + \frac{TN}{\beta}}{RL}\right]^{1/2} \qquad (B24)$$

Again, in the absence of trapping (N = 0), the time constant reduces to the value found in models not including traps: $t = (RL)^{-1/2}$.

We now wish to find an expression for the rise time constant. For this purpose, we start from eq. (B21), including now the illumination term. We thus have:

$$\frac{dn_h}{dt} = (\alpha + 1)\ \frac{dn_t}{dt} = L - R\alpha n_t^{\,2}\ (\alpha + 1) \qquad (B25)$$

and the solution for n_h will be $(\alpha + 1)$ times the solution for n_t, within a constant.

$$\frac{dn_t}{dt} = \frac{L}{(\alpha + 1)} - R\alpha n_t^{\,2} \qquad (B26)$$

$$\frac{dn_t}{dt R\alpha} = \frac{L}{R\alpha\ (\alpha + 1)} - n_t^{\,2} \qquad (B27)$$

Let:

$$\frac{L}{R\alpha\ (\alpha + 1)} = \beta^2 \qquad (B28)$$

$$\frac{dn_t}{\beta^2 - n_t^{\,2}} = R\alpha dt$$

$$R\alpha t = 1/2\ \beta \log \left\{(\beta + n_t)(\beta + n_t)^{-1}\right\} \qquad (B29)$$

$$(\beta + n_t)\ (\beta - n_t)^{-1} = \exp\ \{2\beta R\alpha t\}$$

$$n_t = \beta \left[\left\{ \exp\ (2\beta R\alpha t) - 1 \right\} \left\{ \exp(2\beta R\alpha t) + 1 \right\}^{-1} \right] \qquad \text{(B30)}$$

$$n_h = (\alpha + 1)\ \beta\ \frac{\exp(2\beta R\alpha t) - 1}{\exp(2\beta R\alpha t) + 1} \qquad \text{(B31)}$$

Replacing α and β by their values:

$$n_h = n_{h_o}\ \frac{\exp(4LR\alpha/\alpha + 1)^{1/2} - 1}{\exp(4LR\alpha/\alpha + 1)^{1/2} + 1} \qquad \text{(B32)}$$

where n_{h_o} is the steady state number of holes in the valence band. The rise time constant is therefore of the order of:

$$t \simeq \frac{1}{2}\ \left\{ \frac{\alpha + 1}{LR\alpha} \right\}^{1/2} \simeq\ \frac{1}{2}\ \left\{ \frac{\frac{TN}{E} + 1}{LR} \right\}^{1/2} \qquad \text{(B33)}$$

It is interesting to note that (B33) is identical with (B24) except for a factor of two.

To conclude this discussion, a few words might be added, regarding the temperature dependence of both steady, and transient solutions. The temperature dependence is implicit in the "evaporation constant" "E", which is expected to be proportional to exp $(-e_i/kT)$, where e_i is related to the traps ionization energy. It is readily seen that a decrease in temperature will decrease "E", increasing both time constants and steady state amplitude. Those two quantities are therefore expected to vary exponentially with temperature. We must remember however, that this applies exactly only in the case of our model.

Generally, photoconductors can be either linear, sublinear or superlinear with respect to the illumination (L). The sublinear case will prevail when the rate of illumination is high, while the linear case happens for low light level (low concentration of carriers). We have discussed the sublinear case here. The discussion could be readily extended to the linear case, by assuming in the equations, a low concentration of optically excited carriers.

C. Survey of the Literature

The first investigations on the photoconductivity of cuprous oxide were made by Pfund (1916) on samples containing considerable excess of oxygen. In the same year, Millikan (1916), in his experimental investigation of the Einstein photoelectric equation, determined the long wavelength limit of the photoelectric effect to be 2535 ± 50 Å for cupric oxide (CuO). Nearly the same value was later found for Cu_2O. We mention this to suggest a reason for the peak in the photoconductivity curve between .25 and .30μ found by Pfund and other investigators.

After the initial discovery of photoconductivity by Pfund, the effect was confirmed by the experiments of Coblentz (1922) and Barton (1924).

The more precise study of photoconductivity begins with Schönwald (1932), who introduced the technique of A.C. measurements to eliminate the effect of secondary currents on the primary photocurrents. Schönwald measured the spectral response of cuprous oxide from .56μ in the visible spectrum to about 4 μ in the infra-red. Although there was considerable difference in behaviour among the samples, three peaks in the response were almost always present. The first was close to the absorption edge at .63μ; a second near .8μ, and finally, a much weaker response peaked at 2μ (Fig. 9). By chopping

the incident light at different frequencies, Schönwald also showed that the photoresponse was frequency independent to about 5000 cps at room temperature; he thus estimated the lifetime of the current carriers to be approximately 10^{-5} sec. By focussing the incident light on small areas of the sample, he attempted to associate areas of different response, to visible peculiarities of the sample used. No such association could be found.

In the following year, the carriers of the photocurrent were shown to be of positive polarity by Engelhard (1933), in conjunction with Hall effect measurements he made at low temperatures.

In 1937, Joffe and Joffe (1937) established that the photoresponse was dependent on the thickness of the sample, and noted the absence of the .8μ response at liquid nitrogen temperature. They also showed that the photoconductivity maximum moves to shorter wavelengths for decreasing sample thickness.

Subsequent investigations of photoconductivity, in particular by Russian authors, are mostly concerned with the time constant, and mode of decay of the photocurrent. Studies by Zhuze and Ryvkin (1947) showed that the time constant τ and quantum efficiency η for the photocurrent alter exponentially with temperature as follows: $\tau \propto \exp(\epsilon/2kT)$

$\eta \propto \exp(-\epsilon/2kT)$

where ϵ is $\simeq 0.35$ ev. For instance, according to their results, as the temperature goes from 20°C to - 105°C, τ increases from 1.3×10^{-5} to 0.4 sec. In a later paper (1948), they confirmed the conclusions of Engelhard, as to the positive sign of the carriers. Putseiko (1949), using a condenser method, confirmed that once more, and found no change in the sign of the current carriers throughout the measured spectrum. However, this spectrum was not defined according to the range of wavelengths.

In the next year, Zhuze and Ryvkin (1950) discussed three regions of photosensitivity, centered around .63, .8, and 1.3μ. They also presented evidence for two different regions of behaviour, below -40°C and above -40°C, in the study of A.C. vs stationary photocurrents. In 1952, they proposed a mechanism of the photoconductivity in Cu_2O. The dark conductivity, being due to holes, is caused by thermal electron transitions to excess oxygen impurity levels. The absorbed photon then lifts electrons from the impurity levels into the conduction band, from which they fall into metastable trapping levels below the conduction band (Fig. 10). Light absorption in the Cu_2O absorption band creates excitons which, when in contact with ionized impurity centers, transfer energy and cause an electron transition to the conduction band. It is also stated that one must assume that the recombination of

electron-hole pairs is much greater in the impurity levels than in the trapping levels.

The influence of tempering on the A.C. photoconductivity of Cu_2O has been studied by Okada and Uno (1949). They found that the relative importance of the .8 and .6 μ responses can be influenced by tempering. The .6 μ response is strong for samples with high dark conductivity, and can be increased by heating in oxygen. Annealing in vacuum (10^{-3} mm Hg; 900°C) and quenching down to room temperature resulted in a sample with response at .8μ only.

In an article in the Encyclopedia of Physics, Garlick (1956) gave a summary of the electronic processes in cuprous oxide, together with a simple band model (Fig. 11). He also mentions his own investigations on the spectral response of Cu_2O, where he obtained, in addition to the usual peaks at .6 and .8 μ, a peak at 1.15 μ.

A recent article on the photoconductivity of Cu_2O, by Klier, Kuzel and Pastrnak (1955) is described in the Chemical Abstracts. They found an extra peak at .75 μ, and their .8 μ response was usually greater than the .6 μ response. Their investigations, however, were made on Cu_2O cooled in air, and their samples must therefore have contained considerable excess of oxygen.

From conductivity, photoconductivity and luminescence

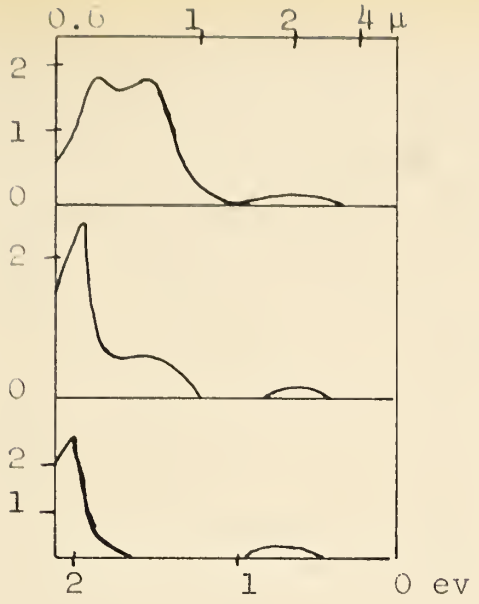

Fig. 9

Typical curves of photoresponse vs wavelength from Schönwald

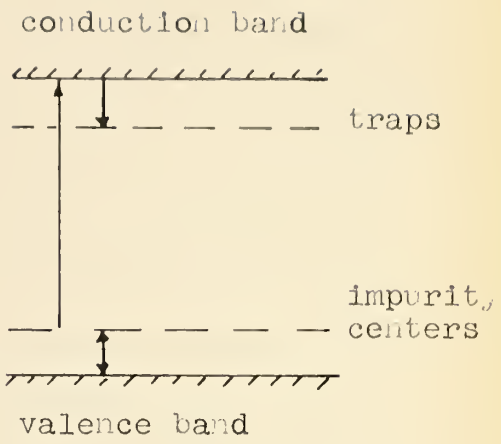

Fig. 10

Photoconductivity scheme from Zhuze and Ryvkin.

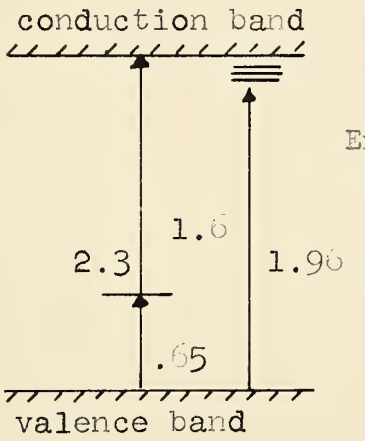

Energy values in ev

Fig. 11

Photoconductivity scheme from Garlick.

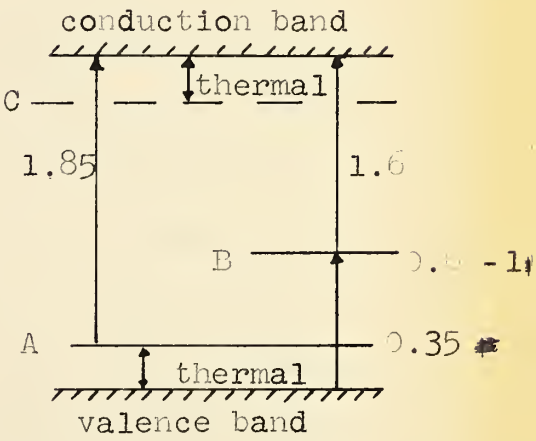

Fig. 12

Photoconductivity scheme from Bloem.

studies, Bloem (1958) proposes an energy level diagram for optical and thermal transitions (Fig. 12) in Cu_2O, together with an identification of the particular impurity levels with certain types of defects. With reference to Fig. 12, levels A and C, according to Bloem, are due to oxygen ion vacancies, which, owing to their effective double positive charge, may bind one or two electrons, giving centers with effective charges equal to plus one and zero respectively. Level A is associated with the plus one center, while level C is assumed to be neutral. Level B, on the other hand, would be due to copper vacancies, the filled level corresponding to a copper ion vacancy Cu+, the empty level corresponding to a neutral Cu atom vacancy. According to this picture, either levels could become emptied or filled up, depending on the possibility of thermal restoration of the equilibrium.

More recently, Weichman (1960) has published the results of his investigations on the photoconductivity of Cu_2O, in relation with its other semiconducting properties. These studies have been performed on high resistivity samples of mosaic structure. The author found that the .6μ peak can be shifted from shorter to longer wavelengths by exposing the sample to low oxygen pressure at 860°C. (Fig. 13) Furthermore, the peak near .8 μ was found to increase in magnitude relative to the others, under these circumstances. This is

A: sample exposed to atmosphere for a few weeks.

B: sample outgassed at 860°C in charcoal trap vacuum and quenched to room temperature.

C: same treatment as in B, but slowly cooled down.

D: heated at 860° under fore pump vacuum.

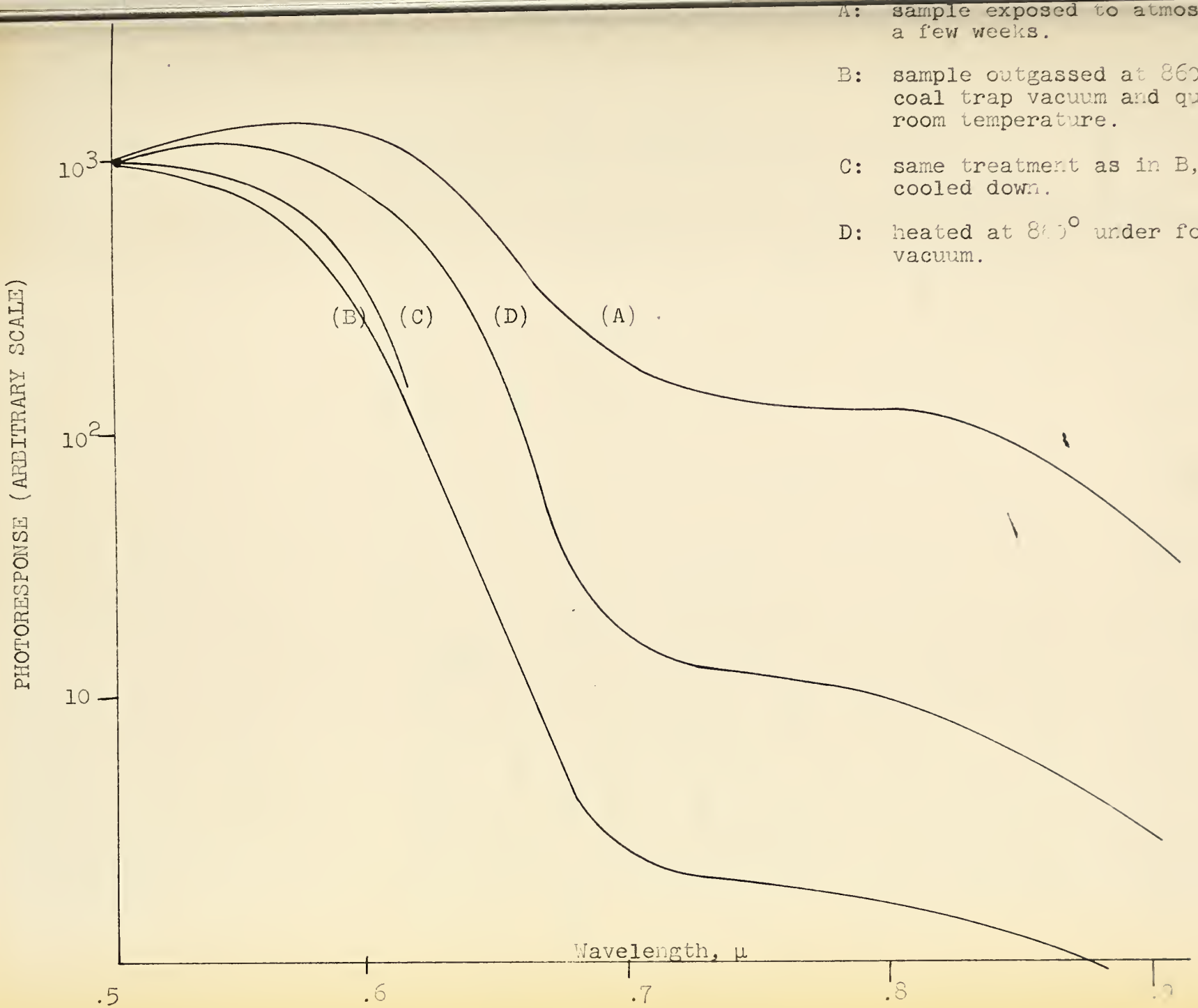

of considerable interest for the present work, since at least one of our samples was of the same type as the ones studied by Weichman, and, as we shall see later, exhibited a similar behaviour.

Finally, to conclude this section, we mention the very recent studies of Pastrnak and Timov (1961) on the spectral distribution of the photoconductivity in Cu_2O. Their work was done at low temperatures, and, as far as we can see, in air. Since they used Blankenburg's and Kassel's (1952) method of crystal growing, it seems quite likely that, what they called "single crystals" ~~is~~ are what we call "mosaic structure crystals". Furthermore, their samples were not defined with respect to their resistivity. Their measurements were taken mostly in the short wavelength region of sensitivity (.44 - .6 μ), where they could find a structure corresponding to the exciton lines found in optical absorption studies. (Apfel and Portis -1960- find the same results in a larger range of temperatures.) They also point out that the time constants increase with increasing λ, and that ~~it~~ they also depend$ on the electrical field applied to the sample.

D. Own Results

Our main object was to determine whether or not single crystals of Cu_2O had strikingly different photoconductive properties, as compared to the polycrystalline material. For this purpose, we investigated the photoconductivity of two kinds of crystals, single and mosaic structure, with respect to their spectral sensitivity at four different temperatures. We also investigated the order of magnitude of the time constants involved, and the dependence of the photocurrent on temperature at a few wavelengths. We tried to keep the oxygen content of the samples as close as possible to the stoichiometric proportions, by outgassing the samples at $1000^{o}C$ in vacuum before sealing them in the holder, and by keeping them under high vacuum during the course of our investigations.

1. General

Our spectral sensitivity curves generally exhibited two maxima, one in the .6 μ region, and one in the .85 μ region. Contrary to previous investigators, we never found any far infra-red response around 2 μ. The results are shown in Fig. 14 and 15 for both mosaic and single crystals, at different temperatures.

Fig. 14 Photoconductivity of the mosaic crystal

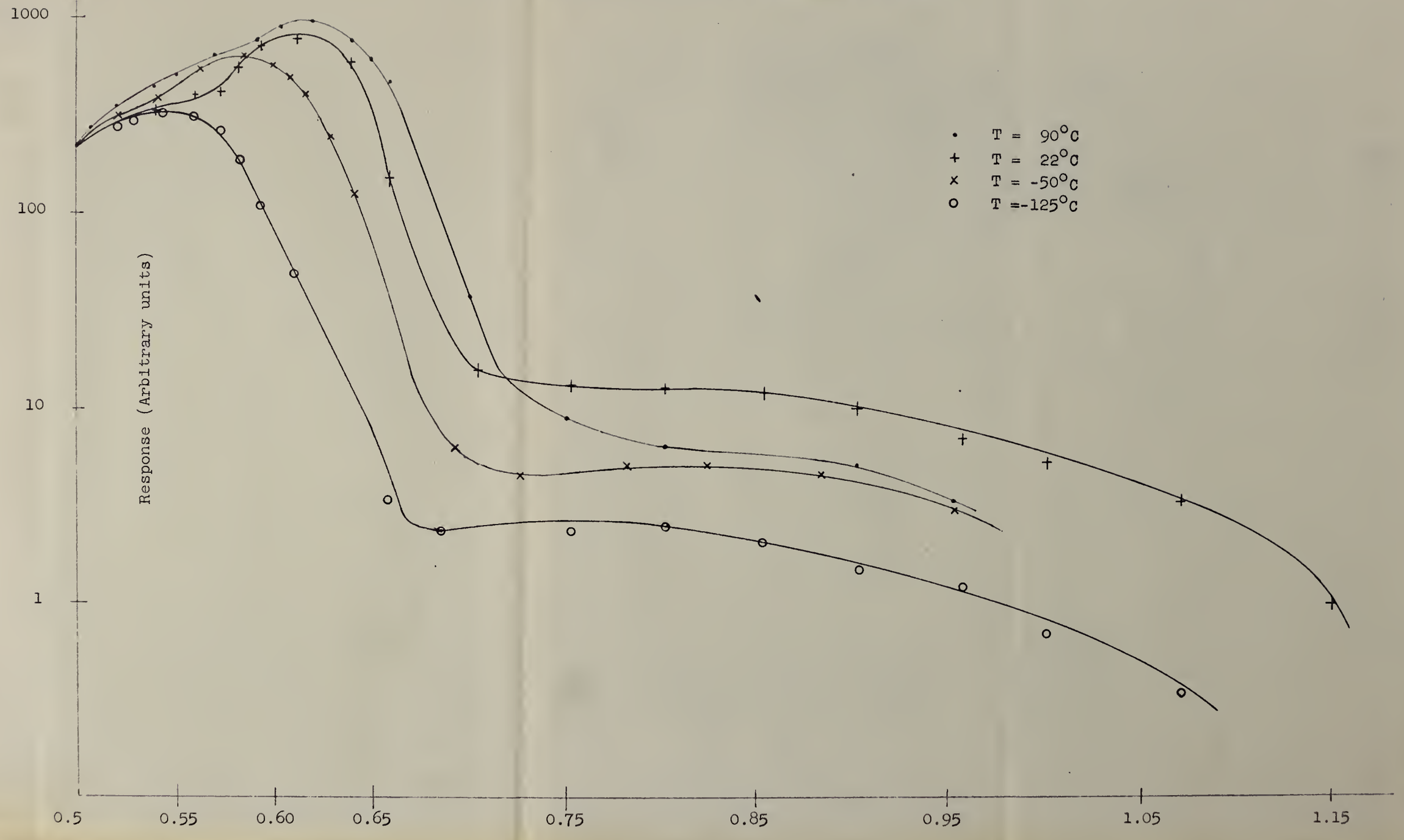

Fig. 15 Photoconductivity of the single crystal

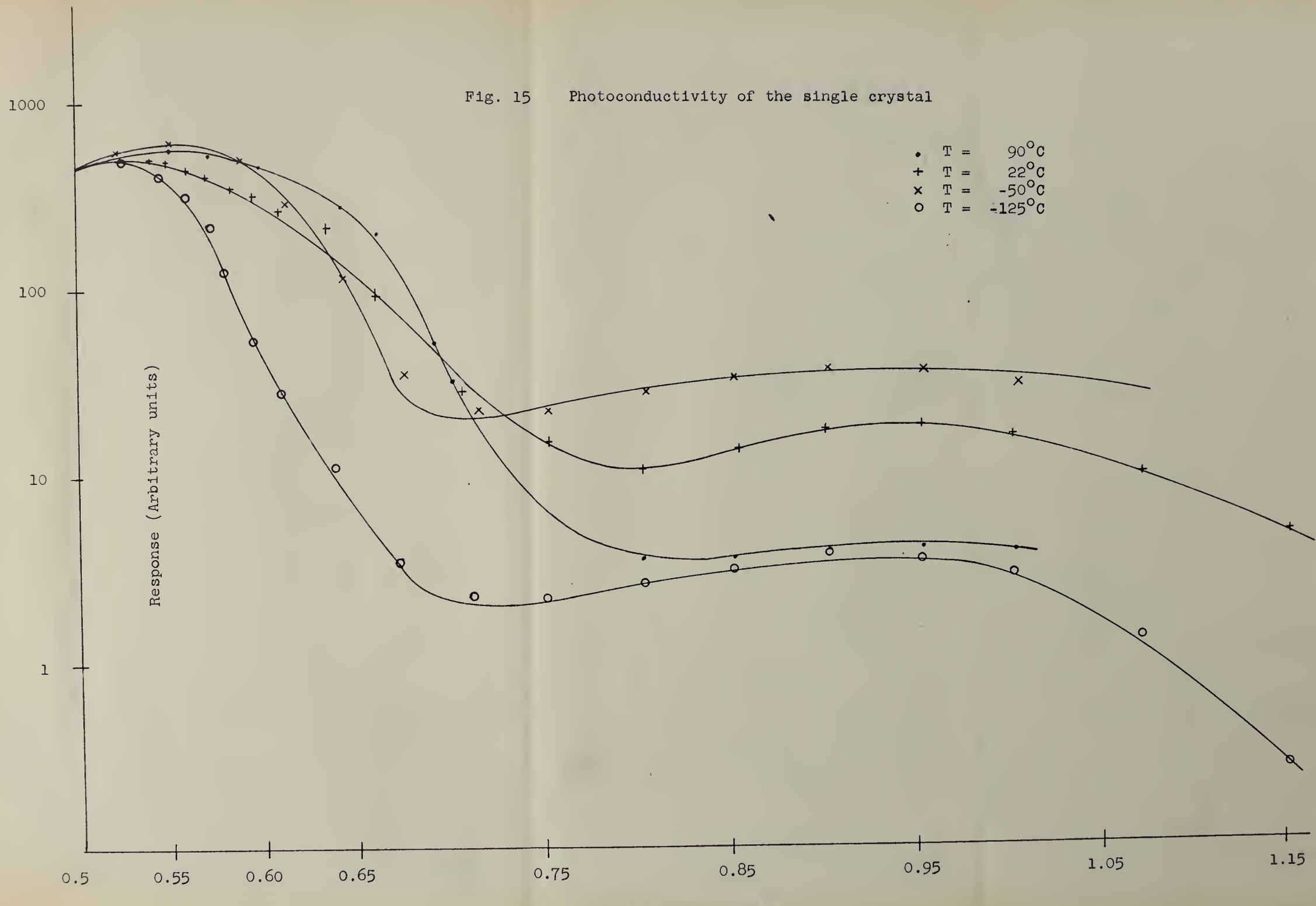

2. Wavelengths of half-response

In table 1, we give the values of the optical activation energies, as determined from the photoconductivity curves according to Moss' formula.

Temperature		-125°C	-5)°C	22°C	9)°C
Single Crystal $\lambda_{1/2}$(ev)	Vis.	2.18	2.)5	1.98	1.95
	I.R.	1.2)	1.2)	1.14	1.1)
Mosaic crystal	Vis.	2.1)	2.))	1.88	1.85
	I.R.	1.30	1.29	1.28	?

Table 1.

$\lambda_{1/2}$ values (ev.) at different temperatures for both types of crystals.

We see that the values found for the main peak correspond fairly well to the values determined by conductivity measurements, for the energy band gap. We therefore conclude that the main peak is due to direct transitions creating electron-hole pairs.

The $\lambda_{1/2}$ found for the infra-red, do not correspond too well to any of the impurity levels found in conductivity measurements. It was here fairly difficult to determine the position of the flat region preceding the decay; besides, the noise level was fairly high as compared to the signal

amplitude. However, if we assume that the infra-red response is due to optical transitions from an impurity level to the valence band, figures check fairly well, energy wise. For instance, in the case of the mosaic crystal, there is an impurity level at .8 ev above the valence band, according to resistivity measurements. Subtracting this value from the band gap, we get a value of about 1.2 ev which corresponds to the $\lambda_{1/2}$ energy for the infra-red.

From the theory, we should also expect that the $\lambda_{1/2}$ values should increase linearly with increasing temperature. An attempt to plot the temperature dependence of the $\lambda_{1/2}$ values showed no such linearity. Due to the scarcity of the points (4 only), only a trend in the expected direction could be found. It must be remembered however, that this linear dependence applies only for $T \gg \theta$, where θ is the Debye temperature. For Cu_2O, θ is of the order of 300°K, so that most of our measurements were taken around the region where the linear dependence no longer applies. However, results are not inconsistent with the value of 3×10^{-4} ev/°C found by Weichman (1950) and others by optical absorption methods.

3. Details of the curves

A more detailed examination of the curves reveals three major points:

a.) our main peaks are shifted towards the ultra-violet, with respect to the position found by other investigators;

b.) the main peak decreases in width as the temperature decreases;

c.) in the case of the mosaic crystal, there is an extra peak at .62 μ.

The first effect has already been observed by previous investigators (see Weichman 1950); they noticed that, the higher the resistivity of the sample, the further the main peak was shifted towards the ultra-violet. This observation seems to be verified here: the single crystal, which had a resistivity ten times greater than that of the mosaic crystal, shows a more pronounced shift towards the ultra-violet. It may be pointed out here, that Cu_2O is an extrinsic semiconductor at room temperature, and therefore, a higher resistivity presumably means a higher purity. On this basis, it is a simple matter to explain the shift of the maximum: it simply means that, per cent wise, impurity transitions play a minor role in the region of the main peak.

The second and third effects can be interpreted by

assuming the presence of a broad acceptor level, situated close to the valence band (possibly the .1 ev level found in conductivity measurements). This assumption is not inconsistent with a suggestion by Bloem (1958); from luminescence studies, he finds such a level at 1.85 ev below the conduction band, and connects it with ionized oxygen vacancies. According to this picture, the .62 μ peak found in the case of the mosaic crystal is due to transitions from this level to the conduction band. At room temperature and higher, this level can easily be replenished by thermal transitions; as one goes down in temperature however, this is no longer possible, and the extra peak gradually disappears: the photoresponse curve becomes slimmer, as the direct band to band transitions become more important, per cent wise.

Further evidence for this model is found in the single crystal response curves. Here, we are dealing with a high resistivity, and presumably purer and more perfect crystal. We thus expect that the "extra peak" near .6μ will be almost non existent. This is found to be the case: the main peak, this time, lies around .55μ, and no extra peak is observed around .6 μ. However, the exponential fall of the response seems to be "retarded" at higher temperatures. This would seem to indicate that the "broad impurity level" is also present in the single crystal, but to a lesser extent.

It may be possible that in the case of previous measurements, the main peak has been completely masked by transitions of the type mentioned here.

Most authors mention an alteration of their .8 μ response at low temperatures. Joffe and Joffe (1937) found that it disappears completely, while Okada and Uno (1949) noticed a marked decrease. For samples cooled in air, Klier et al (1955) found that their samples had a higher response in the .8 μ region than in the .6 μ region. On our own samples, the response around .8 μ remained of the same order of magnitude at all temperatures, and was always smaller than the visible peak by at least two orders of magnitude. Since our crystals were carefully outgassed, and in view of the results of Klier et al on samples presumably containing considerable excess of oxygen, it seems natural to relate the .8 μ response to copper vacancies.

Finally, we should mention that, as expected from the theory, the response goes down at short wavelengths: transitions take place in a very thin layer, and the greater concentration of charge carriers brings about a higher recombination rate.

4. Time constants

Rise and decay times of the photocurrent were measured at the visible and at the infra-red peaks. The values are listed in Table 2.

T	Single Crystal				Mosaic Crystal			
°C	Visible Rise	Visible Decay	Infra-red Rise	Infra-red Decay	Visible Rise	Visible Decay	Infra-red Rise	Infra-red Decay
90	.2	.3	.12	.1	.2	.3	.2	.4
22	1	2	1	2	.8	1.6	2.5	3.5
-50	2	4	2	4.5	2.5	1.6	4	6
-125	2	4	2	4	1.4	1.6	1.4	3

Table 2.

Rise and Decay Time Constants (Milliseconds).

According to previous investigators (Ryvkin 1948), the time constants should vary exponentially with temperature. Our results show no such simple dependence. At the best, only a trend can be determined: the time constants increase with decreasing temperature up to a point, where a reversing effect seems to set in; also, the rise is usually faster than the decay, and finally, the infra-red is slower than the visible. We propose to give a detailed explanation of the observed time constants, in connection with a proposed model.

We must mention however, that our method of measurements, did not permit us to observe any long time constant effects. We chopped the light at forty cps, and defined the time constant as the time required for the observed signal to reach 63% of its maximum value. But throughout the investigation, it became more and more apparent that two different time constants were involved: a fast one, responsible for most of the signal measured during the cycle, and, mainly at low temperatures, a much slower one giving a response which our A.C. arrangement did not measure. Our equipment therefore measured the faster time constant, which is presumably connected with transitions from the vicinity of the valence band. The longer time constant involves electron trapping near the conduction band and is therefore expected to be strongly temperature dependent. Further evidence in support of that idea was found in D.C. photoconductivity measurements at low temperatures. The spectral sensitivity curve was found to be similar to the A.C. curve, but a much longer time constant was observed (of the order of a second or two). This would correspond more closely to the value of 0.4 seconds found by Ryvkin (1948) at - 105°C.

5. Proposed model

A simple model is now proposed for the Cu_2O photocon-

ductive transitions. Qualitatively, this model is quite similar to the models proposed by Bloem, Garlick, Weichman and others. Only the position of the levels, which seems to vary from author to author, is, once again, different.

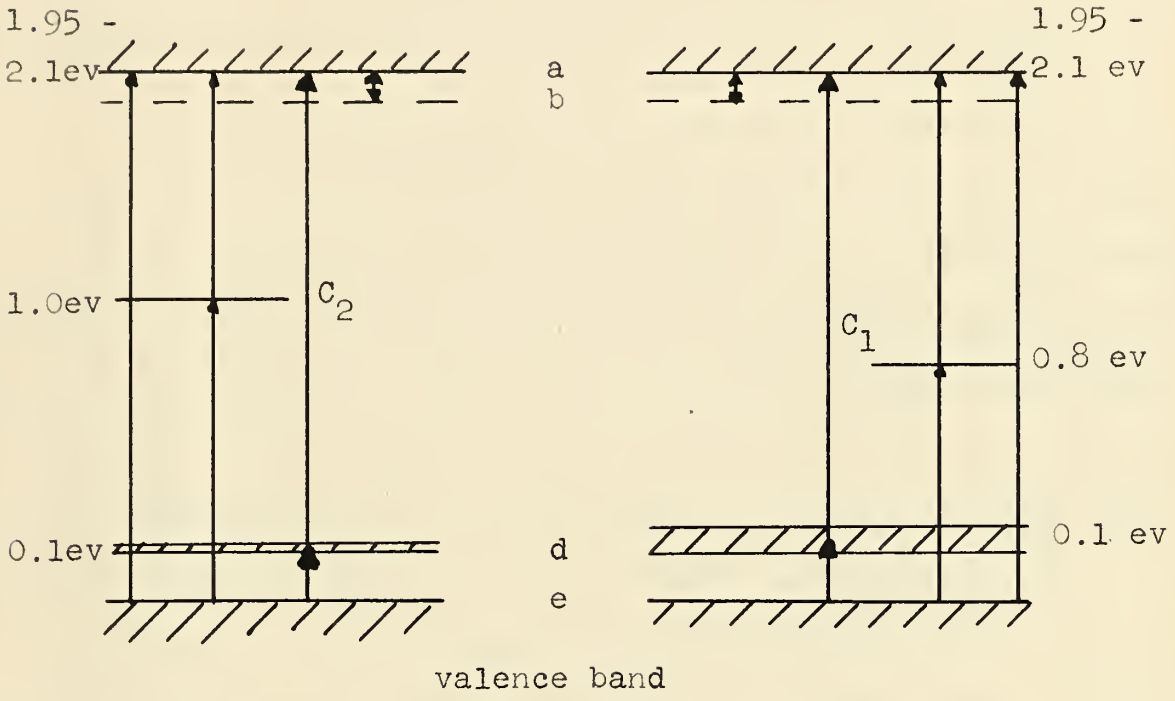

Fig. 16

Photoconductive transitions in Cu_2O.

Left: single crystal;

Right: mosaic crystal.

In Fig. 1[illegible], a represents the bottom of the conduction band, e, the top of the valence band; b is a trapping level situated somewhat below the conduction band. The c's are deep lying impurity levels: c_1 (.8 ev) in the case of the mosaic crystal, c_2 (1.0 ev.) in the case of the single crystal; d is the "broad level" which we have mentioned previously. We now intend to discuss the photoconductivity curves, and the time constants in terms of that model.

At high temperatures, the response in the visible is due to e → a transitions (as indicated by the $\lambda_{1/2}$ values) and in the region of the "extra peak", d → a transitions also exist, the latter being dominant, and thermal excitations e → d keeping d full. The level d is shallower in the single crystal (higher purity), and in this case, d → a transitions are less important in this region. The time constants of the visible response at high temperatures will be fast (approaching the lifetime of a free carrier), the e → a transitions equilibrium being quickly established. The d → a transitions take longer to reach an equlibrium, (since they involve thermal transition equilibrium) so that the overall time constant can be expected to increase as the wavelength is increased. This is actually found to be the case.

Energy-wise, the infra-red response has to be assigned to c → a and e → c transitions as well. The response peaks in

the .8 μ - .9 μ range, as already found by previous investigators.

At low temperatures, the photoresponse features the disappearance of the "extra peak", in the case of the mosaic crystal. Level d empties out, and cannot be replenished by thermal transitions any more. Since the "extra peak" is still present at - 50°C, the d level is expected to be fairly close to the band edge, and may coincide with the .10 ev level found in resistivity measurements.

The time constants that we measured, involved the establishment of thermal equilibrium between levels e and d; at high temperatures, this equilibrium is quickly established and does not affect the time constants to a large extent. As the temperature goes down however, thermal equilibrium is slower at level d: therefore, the time constants increase. As the temperature goes down further, thermal transitions from the valence band to level d are no longer possible, and level d empties out, the faster transitions e → a slowly takes over, per cent wise: the time constants level off, and even decrease. As mentioned before, trapping occurs at level b, but the resulting long time constants found in D.C. measurements, were eliminated by our A.C. equipment.

Infra-red response, at low temperatures, comes essentially from the same process as for high temperatures. At -125°C, it was noted that D.C. illumination with visible light, in-

creased the response by a factor of two. This indicates that in the infra-red case, the $\underline{c} \rightarrow \underline{a}$ transitions are dominant: as the temperature decreases, level $\underline{c}$ empties out; the D.C. illumination plays roughly the same role as "heat" in re-establishing the number of electrons in $\underline{c}$, which, according to this hypothesis, acts as a trapping level at low temperatures. This idea has been supported by Weichman (1959), on the basis of photoconductivity and luminescence studies.

IV. CONCLUSION

The main purpose of this investigation was to study the photoresponse of single crystals of cuprous oxide, in the visible and near infra-red spectrum. For this purpose, single crystals were grown and analyzed by X-ray diffraction methods. A mosaic structure crystal was also studied for sake of comparison.

From conductivity measurements at room temperatures, a new acceptor level was found at 0.1 ev above the valence band. This level is believed to be responsible for the enhancement of the photoresponse in the 0.6 μ region of the spectrum. It was also shown that the behaviour of the time constants was consistent with the existence of such a level.

Activation energies, as obtained from photoconductivity curves, coincide with the values found from conductivity measurements, as predicted by the theory. Also, the temperature dependence of these activation energies ~~were~~ was found to be consistent with the temperature dependence of the optical absorption edge.

Finally, we have seen that single crystals exhibit the same general behaviour as polycrystalline samples. It seems reasonable to conclude that two samples of equal degree of purity, will react in a similar way to optical excitations, quite independently of their structural perfection.

If such a dependence exists, it is largely overshadowed by the presence in the lattice of excess copper or excess oxygen.

Other aspects of the photoresponse are currently under investigation: for instance, the variation of the photocurrent amplitude ~~in~~ with the temperature. Details are still incomplete, but the photocurrent seems to decrease exponentially with decreasing temperature, at all wavelengths. Such investigation -- it is hoped -- will yield a greater insight into the complex behaviour of cuprous oxide.

BIBLIOGRAPHY

ANDERSON, J.S. and GREENWOOD N.W., Proc. Roy. Soc. 215A, 353 (1952).

APFEL, J.H. and PORTIS A.M., Phys. Chem. Sol. 15, 33 (1960).

BARDEEN, J. and SCHOCKLEY, W., Phys. Rev. 80, 72 (1952).

BARTON, A.W., Phys. Rev. 23, 337 (1924).

BLANKENBURG, G. and KASSEL, K., Ann. d. Phys. 10, 201 (1952).

BLOEM, J., Philips Research Repts 13, 167 (1958).

BÖTTGER, O., Ann. d. Phys. 10, 232 (1952).

COBLENTZ, W.W., U.S. Bureau of Standards, Sc. Publ. 18, 603 (1922)

CULLITY, B.D., Elements of X-ray Diffraction. Addison Wesley Publ. (1956).

ENGELHARD, E., Ann. d. Phys. 17, 501 (1933).

FAN, H.Y., Phys. Rev. 82, 900 (1951).

GARLICK, J.F.G., Ency. of Phys. 19, 377 (1956)

GUDDEN, B. and POHL, R.W., Z. f. Phys. 17, 331 (1923)

JOFFE, A.W. and JOFFE, A.Th., Phys. Z. d. Sov. Un. 11, 241 (1937).

JUSE, W. and KURTSCHATOV, B.W., Phys. Z. d. Sov. Un. 2, 953 (1932).

KLIER, E., KUZEL, R. and PASTRNAK, J., Czech. J. of Phys. 5, 421 (1955). Chem. Abs. 50, 5397i (1956).

MILLIKAN, R.A., Phys. Rev. 7, 18 (1916).

MOSS, T.S., Photoconductivity in the Elements N.-Y. Academic Press (1952). Proc. Phys. Soc. B62, 741 (1949b).

MOTT, N.F. and FRÖHLICH, H., Proc. Roy. Soc. (London) 171, 496 (1939).

OKADA, T. and UNO, R., J. Phys. Soc. Japan 4, 351 (1949).

O'KEEFE, M. and MOORE, W.J., J. Chem. Phys. 35, 1324 (1961).

PASTRNAK, I. and TIMOW, R.A., Sov. Phys. Sol. State 3, 627 (1961).

PFUND, A.H., Phys. Rev. 7, 289 (1916).

PUTSEIKO, E.K., Dokl. Akad. Nauk. USSR 67, 1009 (1949).

ROSE, A., R.C.A. Rev. 12, 362 (1951)

Photoconductivity Conference, p. 11 - John Wiley & Sons N.-Y. (1954)

SCHÖNWALD, B., Ann. Phys. Lpz. 15, 395 (1932).

TOTH, R.S., KILKSON, R., TRIVICH, D., J. App. Phys. 31, 1117 (1960).

Phys. Rev. 122, 482 (1961).

WEICHMAN, F.L., Phys. Rev. 117, 998 (1960).

Thesis: The electrical and optical properties of Cu_2O; Northwestern U., June 1959 (unpublished).

ZHUZE, V.P. and RYVKIN, S.M., Dokl. Akad. Nauk. USSR 58, 1629 (1947)

62, 55 (1948)

Izvest. Akad. Nauk. Ser. Fiz. 16, 93 (1952).